Supporting Information

Serine 85 functions as a catalytic acid in the reprotonation process during EvAS-catalyzed astellifadiene biosynthesis

Weiyan Zhang,[a] Kaitong Peng,[a] Keying Lan,[a] Kangwei Xu,[b] Ruibo Wu,[b] Tom Hsiang,[c] Shaoping Nie,[d] Lixin Zhang,[a] Xinye Wang,[a,e] and Xueting Liu*[a]*

Correspondence

Xueting Liu, State Key Laboratory of Bioreactor Engineering, and School of Biotechnology, East China University of Science and Technology (ECUST), Shanghai 200237, China.

E-mail: liuxueting@ecust.edu.cn (X. Liu); xywung@163.com (X. Wang).

Table of Contents

Supplemental Materials and Methods

1.1. General

Oligonucleotide synthesis and DNA sequencing were performed by Tsingke (Beijing, China). The plasmid preparation kit I (D6943-02) was obtained from Omega Bio-tek (Norcross, GA, USA), and the ClonExpress II One Step Cloning Kit was purchased from Vazyme Biotech Co., Ltd. (Nanjing, China). All commercial chemicals were acquired from Sigma (Saint Louis, MO, USA), Takara (Otsu, Japan), Adamas-beta (Shanghai, China), or Sinopharm Chemical Reagent (Shanghai, China). Semipreparative HPLC was conducted using a ZORBAX SB-C18 column (10 × 250 mm, 5 μm). The ^{1}H, ^{13}C, and 2D NMR were recorded on an Agilent DD2 (Santa Clara, CA, USA) 600 MHz NMR spectrometer. The NMR spectra were referenced to solvent signals with resonances at δ_H 7.16 ppm, δ_C 128.06 ppm in C_6D_6, and δ_H 7.26 ppm, δ_C 77.1 ppm in $CDCl_3$. Circular dichroism (CD) spectra were recorded on a Chirascan circular dichroism spectrometer using methanol as the solvent. High-resolution electron ionization mass spectrometry (HR-EI-MS) measurements were obtained using a Waters GCT Premier mass spectrometer. All fermentation biomass was collected using an Avanti JXN-26 centrifuge (Beckman Coulter, USA). Gas chromatography-mass spectrometry (GC-MS) analyses were performed on a Shimadzu GC-2010 Plus connected to a Shimadzu GCMS-QP2010 SE gas chromatograph-mass spectrometer with a DB-5 ms column (30 m × 0.25 μm × 0.25 mm, Shimadzu, Japan).

1.2. Sequence alignment and structure-function relationships of BFTPSs

Protein BLAST analyses were conducted using the Swiss-Prot database at http://www.ncbi.nlm.nih.gov/BLAST. ClustalW was employed to generate a multiple sequence alignment, which was then analyzed and visualized using ESPript 3.0 (https://espript.ibcp.fr/ESPript/cgi-bin/ESPript.cgi). The candidate gene *EvAS* was identified in the genome of *Emericella variecolor* NBRC 32302 (GenBank accession number: LC113889), as retrieved from the NCBI protein database (Table S1).[1] The *EvAS* gene was codon-optimized and synthesized by Tsingke (Beijing, China).

1.3. Structural analysis of EvAS-TC domain

Predictive modeling of the terpene cyclase (TC) domain of EvAS was performed using AlphaFold2.[2] Based on the crystal structures of the fungal sesterterpene synthases NfSS (PDB ID: 8yla) and PbSS (PDB ID: 8yl9),[3] three Mg^{2+} ions and PPi groups from these structures were incorporated into the EvAS-TC model. The active site of EvAS-TC was analyzed using POVME,[4] and amino acids within 5 Å of the active site were selected. Excluding amino acids involved in Mg^{2+} coordination from conserved motifs, eight key residues were identified: I66, S85, F89, F187, W188, S303, N307, and W310.

1.4. Plasmids construction and site-directed mutagenesis

The gene encoding *EvAS* was subjected to codon optimization and synthesis before being cloned into shuttle vectors (pXW55) designed for *Saccharomyces cerevisiae* (*S. cerevisiae*). The gene was then expressed in *S. cerevisiae* strain BJ5464.[5] Putative active sites in the catalytic pocket were targeted for mutagenesis using the pXW55-*wt* plasmid. Table S8 lists the primers used for constructing the mutation libraries of EvAS. Mutations were

introduced into the *EvAS* gene within the pXW55 vector via site-directed mutagenesis using PCR. The PCR reaction system is as follows:

pYET-XW55-EvAS-*wt*	< 50 ng
Primer F	0.2 μM
Primer R	0.2 μM
PrimeSTAR MAX DNA Polymerase	5 μL
ddH2O	4.6 μL
Total	10μL

PCR amplification was conducted using PrimeSTAR® MAX DNA Polymerase (Takara) in a three-step reaction, using the following program: 98 °C, 30 s; (98 °C, 10 s; 60 °C, 15 s; 72 °C, 55 s) × 30 cycles; 72 °C, 5 min. After amplification, the DNA was combined with 2 μL of 6x DNA Loading Buffer and analyzed by electrophoresis on a 1% agarose gel containing DuRed nucleic acid dye. The gel was run at 125 V for 40 minutes. After electrophoresis, the gel was imaged to verify the presence of the target bands. To enhance amplification, the PCR reaction volume was increased to 50 μL while maintaining the same conditions as the 10 μL reaction. Subsequently, the PCR products were digested with a plasmid template, purified, and subjected to homologous recombination. Plasmid sequencing confirmed the successful incorporation of the desired mutations. Subsequently, the plasmid containing the mutated *EvAS* genes were transformed into *E. coli* DH10b.

1.5. Transformation of *S. cerevisiae* expressing wild-type EvAS and its variants

The reconstructed plasmids pXW55-EvAS and its variants were introduced into *S. cerevisiae* strain BJ5464.[5] The procedure for *S. cerevisiae* strain BJ5464 homologous recombination using the Yeast Transformation II Kit (ZYMO RESEARCH) is as follows: i) Thaw the competent cells at room temperature; ii) Add 0.2−1 μg (up to 5 μg) of the reconstructed plasmids to 50 μL of competent cells, then add 500 μL of EZ 3 solution and mix thoroughly by vortexing; iii) Incubate at 30°C for 45 minutes, gently vortexing every 2−3 minutes during incubation; iv) Spread the transformation mixture evenly on the agar plates and incubate at 30°C for 2−4 days. After plating, colonies were picked for protein overexpression, and then cultured in 5 mL of uracil-dropout medium (20 g/L glucose, 5.0 g/L casamino acids, 0.02 g/L adenine, 6.7 g/L YNB, 0.02 g/L tryptophan, pH 7.5) at 30°C with shaking at 220 rpm for 48 hours. Subsequently, 1 mL of the culture was transferred to a 250 mL flask containing 50 mL of YPD medium (20 g/L tryptone, 10 g/L yeast extract, 20 g/L glucose, pH 7.5), and fermentation proceeded at 30°C with shaking at 220 rpm for 3 days.

1.6. Metabolites analysis by GC-MS

After centrifugation to collect the cell pellets from the small-scale culture, the cells were disrupted with acetone and sonicated for 45 minutes. The resulting cell extract was then concentrated under vacuum. The residues were reconstituted in a mixture of water and ethyl acetate. The ethyl acetate-soluble fraction was evaporated under vacuum to yield crude extracts. These extracts, dissolved in ethyl acetate at a concentration of 1 mg/mL, were analyzed using GC-MS. The GC-MS analysis was performed using a DB-5ms column (30 m × 0.25 mm i.d., 0.25 μm film thickness, Shimadzu) under the following conditions. The inlet pressure was set to 110 kPa, and the injection volume was 1 μL. The sample was injected at 60 °C in split mode. The column temperature was initially increased at a rate of 25 °C/min to 280 °C, then further increased at 10 °C/min to 310 °C, where it was held isothermally for 6

minutes. The flow rate of helium carrier gas was maintained at 1.77 mL/min. The mass spectrometry (MS) settings were as follows: source temperature of 200 °C, transfer line temperature of 250 °C, and electron energy of 0.4 kV.

1.7. Isolation and purification of compounds 1 and 2

After a 10 L fermentation of *S. cerevisiae* expressing EvAS-WT, the biomass was collected by centrifugation at 4500 rpm for 10 minutes, yielding 240 g. The biomass was then subjected to three 45-minute ultrasonication treatments with acetone at room temperature, followed by extraction with ethyl acetate. The ethyl acetate extract was concentrated under vacuum, producing a crude extract weighing 0.8 g. This crude extract was fractionated using a silica gel column, resulting in fractions A–D. Fraction A was further purified using semipreparative HPLC with 100% acetonitrile on a ZORBAX SB-C18 column, leading to the isolation of compounds **1** (7.0 mg) and **2** (3.0 mg).

Approximately 25 g (wet weight) of biomass was obtained from the 1 L fermentation of *S. cerevisiae* expressing EvAS-S85N. The biomass was subjected to three 45-minute ultrasonication treatments with acetone at room temperature, followed by extraction with ethyl acetate. The resulting ethyl acetate extract was concentrated under vacuum, yielding 90 mg of crude extract. This crude extract was then fractionated using a silica gel column with hexane as the eluent, producing three fractions (Fr. 1−3). Fraction 1 was further purified by semipreparative HPLC on a ZORBAX SB-C18 column with isocratic elution of 100% acetonitrile, resulting in the isolation of compound **2** (0.9 mg).

1.8. Computational details for DFT calculations

The conformational analysis of compound **2** was performed using the MMFF94 molecular force field and a random search approach in SYBYL X 2.1 software. All conformers within a 10 kcal/mol energy range were identified and further optimized using the B3LYP/6-31G(d) level in the gas phase with Gaussian 09.[6] Conformers with a population exceeding 0.1% were then subjected to electronic circular dichroism (ECD) and specific optical rotation calculations. The ECD spectra were computed using the B3LYP/6-31G(d,p) method in a methanol environment. The simulated ECD curves were weighted according to the Boltzmann distribution of individual conformers. The specific optical rotations were calculated at the B3LYP/6-311G(d,p) level in chloroform using the PCM model at different wavelengths. The calculated specific optical rotation values were then averaged according to the Boltzmann distribution theory and relative Gibbs free energy.[7]

The molecular geometries of compound **2**, with a truncated serine, were optimized using density functional theory (DFT) at the B3LYP/6-31G(d) level. Frequency calculations at the same level of theory were performed to classify all stationary points as minima or transition states. Intrinsic reaction coordinate (IRC) analysis confirmed that all stationary points were smoothly connected. Single-point energies were computed using the mPW1PW91/6-311+G(d,p) method. Gibbs free energies for discussion were derived by adding gas-phase Gibbs free energy corrections obtained at the B3LYP/6-31G(d) level. All calculations were conducted using Gaussian 09.[6]

1.9. Molecular dynamic simulations

Starting structures and system setup

The protein structures of the TC domains of NfSS and EvAS were predicted using AlphaFold2 (Fig. S18).[2] The predicted structure of NfSS was highly consistent with its crystal structure (PDB ID: 8yla), with a root-mean-square deviation (RMSD) of 0.581 Å for structure superposition and a TM-score of 0.956.[8] PROCHECK results indicated that the EvAS model, predicted using AlphaFold2, had a high score (Fig. S19). Consequently, this model was deemed suitable for further studies of EvAS. The TC domain of the EvAS model was reconstructed with the PPi group and a coordination shell of three Mg^{2+} ions, based on the crystal structure of NfSS (sequence similarity: 35.6%; identity: 19.4%). The models of EvAS, EvAS-S85A, EvAS-S85N, EvAS-S85D, and EvAS-S85Y were reconstructed in the same manner. According to the proposed reaction mechanism for astellifadiene (**1**) in EvAS (Fig. S2),[1] intermediates **IM2** and **2** were docked into EvAS using AutoDock Vina.[9] A semi-flexible docking approach was employed to thoroughly sample conformations, accommodate flexibility, and investigate ligand-binding modes. Side chains of residues I66, S85, F89, F187, W188, S303, N307, and W310 were treated as flexible. The search grid box (25 × 25 × 25 $Å^3$) was centered on the substrate-binding site, with an exhaustiveness setting of 64 and default options for other parameters. Finally, nine potential poses were identified from the docking results. The most rational and low-energy conformation was selected as the initial configuration for molecular dynamics simulations (MD). The protein and ions were parameterized using the Amber ff14SB[10] force field, and water molecules were assigned the TIP3P[11] model. Ligand force field parameters were generated with the GAFF force field,[12] with partial atomic charges derived from restrained electrostatic potential (RESP)[13] calculations based on HF/6-31G(d) in Gaussian 09.[6] The complexes were solvated in a truncated octahedral water box, extending 10.0 Å in each dimension, with Na^+ ions added to neutralize the system. Initial coordinates and topology files were generated using the tleap program in AMBER20.

MD simulations

MD simulations of apoproteins and receptor-ligand complexes were conducted with the AMBER20 package.[14] Initially, all atoms of the protein, ligand, and Mg^{2+} were fixed, with only the water molecules free; subsequently, the protein backbone, ligand, and Mg^{2+} were restrained. The system underwent routine minimization, leading to the formation of a protein-ligand complex with preliminary solvent relaxation. The complex was then gradually heated from 0 to 300 K under the NVT ensemble for 50 ps, followed by 100 ps of density equilibration under constant pressure without restraints. Finally, MD simulations were performed for 2 × 100 ns at 300 K, using the SHAKE algorithm to constrain covalent bonds involving hydrogen and the Particle Mesh Ewald (PME) method for long-range electrostatic interactions, with computations accelerated by GPU in the Amber 20 PEMED package.[14]

1.10. Structural elucidation of compounds 1 and 2.

GC-MS analysis of compound **1** identified characteristic ion fragments at *m*/*z* 109, 161, 203, and 325 (Fig. S27A), along with a molecular ion peak at *m*/*z* 340, confirming its classification as a sesterterpene. The ^1H, ^{13}C, and HSQC NMR spectra (Figs. S4–S6, Table S2) displayed distinct resonances for five methyl groups, closely resembling those in astellifadiene synthesized by EvAS,[1] thereby confirming that compound **1** is astellifadiene.

GC-MS analysis of the extract from the transformant containing the *EvAS* gene identified a new metabolite, compound **2**, with an *m*/*z* of 340 (Fig. S27B). Based on the mass spectrum, we hypothesized that compound **2** is a novel sesterterpene hydrocarbon.

Compound **2** was isolated as colorless oil, $[\alpha]_D^{30}$ + 152.0 (c 1.25, $CHCl_3$). The molecular formula of compound **2** was determined to be $C_{25}H_{40}$ from its HR-EI-MS data (*m/z* 340.3124 $[M]^+$; calculated for $C_{25}H_{40}^+$, 340.3130). The ^1H and ^{13}C NMR spectra of **2** in C_6D_6 (Figs. S8–S9, Table S3) showed signals consistent with two olefinic methines, an exomethylene, and five methyl groups, which are typical of a sesterterpene core scaffold. The presence of six degrees of unsaturation and six olefinic carbons in compound **2** suggests a tricyclic ring system.

The COSY spectrum of **2** revealed four spin systems of H-1/H-2, H-4/H-5/H-6, H-8/H-9/H-10/H-14/H-18/H-17/H-16, and H-12/H-13 (Fig. S11). In the HMBC spectrum, key correlations from the methyl signals were observed, as follows: H_3-20 (δ 1.47) to C-2, C-3, and C-4; H_3-21 (δ 1.45) to C-6, C-7, and C-8; H_3-22 (δ 0.85) to C-10, C-11, C-1, and C-12; H_3-23 (δ 0.87) to C-13, C-14, C-15, and C-16; H_3-25 (δ 1.70) to C-18, C-19, and C-24 (Fig. S12). These cross signals confirmed the connections of C-3 to C-2, C-4, and C-20; C-7 to C-6, C-8, and C-21; C-11 to C-1, C-10, C-12, and C-22; C-15 to C-13, C-14, C-16 and C-23; and C-19 to C-18, C-24, and C-25. Furthermore, the HMBC correlations of H-24a (δ 4.77) and H-24b (δ 4.70) to C-18 and C-19 established the connections of C-18 to C-19, which defined the planar structure of **2** as a type B sesterterpene with a 5/6/11 tricyclic system (Fig. 2B). Comparative analysis of the ^1H and ^{13}C NMR spectroscopic data in $CDCl_3$ of **2** with those of **C1** produced by AtTPS06 from *Arabidopsis thaliana*[15] suggested structural similarities between them (Table S4). The relative stereochemistry of **2** was determined mainly by NOESY correlations (Fig. S13). The configurations of $\Delta^{2,3}$ and $\Delta^{6,7}$ double bonds were established as 2*E*,6*E* by the correlations of H-2 and H-4, as well as H-6 and H-8. The relative configurations of 10*S**,11*R**,14*S**,15*S**,18*S** were determined from the correlations between H-10 and H-23/H-18, H-18 and H-23, and H-14 and H-22/H-25. The absolute configuration of compound **2** was confirmed using time-dependent density functional theory (TD-DFT) to estimate its theoretical ECD curve at the B3LYP/6-31G(d,p) level. The simulated ECD spectrum matched the experimental spectrum, verifying the stereochemical assignments of 2*E*,6*E*,10*S*,11*R*,14*S*,15*S*,18*S* for compound **2** (Fig. S17). Thus, the absolute configuration of compound **2** was confirmed as 2*E*,6*E*,10*S*,11*R*,14*S*,15*S*,18*S*-**2**, an enantiomer of **C1**. Unfortunately, the specific optical rotation of the *A. thaliana* compound **C1** was not reported in the literature, as only 0.6 mg of the compound was isolated, which precluded its measurement. Therefore, a direct comparison of optical rotations could not be made. To further support our assignment, we calculated the optical rotation of compound **2** at different wavelengths using the B3LYP/6-311G(d,p) level in chloroform with the PCM model. The overall calculated optical rotation is positive (Table S5), closely matching the experimental value. These results confirm the absolute configuration of compound **2**, identifying it as the previously uncharacterized sesterterpene astellifatriene.

1.11. Protein sequence of EvAS (accession number: LC113889)

MEFKYSTLIDPEMYETEGLCDGIPVRYHNNPELEEIDCLRCHEHWRENVGPLGVYKG
GLADQWNGISIAIPEALPDRLGVVSYASEFAFVHDDVIDIAQHGNEQNDDLRVGFEQ
MIDAGAIKYSTSGKRALQSYIAKRMLSIDRERAIISLRAWLEFIEKTGRQEERRFNNEK
EFLKYRIYDVGMLFWYGLLTFAQKITIPENELTTCHELAIPAYRHMALLNDLVSWEK
ERASSIALGKDYCINFIFVAMEESGISEDEAKERCREEIKLATVDYLRVFDEAKDRIDL
SHDTMLYLESLLYSMSGNVVWGLQSPRYYTDAKFSQRQLDWIKNGLPLEVRLEDRV

FGLSPSEDRVTHQAVIENGLPESGLGKNGNSSNGVDVNKALLSAVLHEHLKGHAVF
KMSDHEVKVKASNGRSLDTKVLQAPYEYITGLPSKRLREQAIDAMNVWFRVPAEKL
DLIKSITTILHNASLMLDDVEDGSELRRGNPSTHTIFGLSQTINSANYQLVRALERVQK
LEDSESLLVFTEELRNLYIGQSMDLYWTGNLICPTMNEYFHMVECKTGGLFRLFTRL
MSLHSTSAVKVDPTTLSTRLGIYFQTRDDYKNLVSTEYTKQKGYCEDLEEGKFSLPLI
HLIQAMPDNHVLRNILTQWRVTRKVTLAQKQVVLGLMEKSGSLKFTRETLASLYSG
LEKSFTELEEKFGTENFQLKLILQFLRTE

1.12. DNA sequence of codon-optimized *EvAS* (opt)

ATGGAATTCAAGTACTCCACTCTGATCGACCCGGAAATGTACGAAACCGAAGGT
CTGTGTGACGGTATCCCAGTTCGCTACCACAACAATCCGGAACTGGAAGAAATC
GACTGCCTGCGTTGCCACGAACACTGGCGTGAGAACGTTGGTCCGCTGGGTGTTT
ACAAAGGTGGTCTGGCAGACCAGTGGAACGGTATCTCTATCGCGATTCCAGAAG
CTTTGCCGGACCGTCTGGGTGTTGTTAGCTACGCTTCCGAATTCGCGTTCGTTCAT
GACGACGTTATCGACATCGCACAGCATGGTAACGAACAGAACGACGATCTGCGT
GTTGGTTTCGAACAGATGATCGATGCGGGTGCAATCAAATACTCTACCTCCGGTA
AACGTGCTCTGCAGTCTTACATCGCTAAACGTATGCTGTCTATCGACCGTGAACG
TGCGATCATCTCTCTGCGTGCTTGGCTGGAATTCATCGAAAAGACCGGTCGTCAA
GAAGAACGTCGTTTCAACAACGAGAAAGAATTCTTGAAATACCGTATCTACGAT
GTTGGTATGCTGTTCTGGTACGGTCTTCTGACTTTCGCTCAGAAAATCACCATTCC
GGAGAACGAACTGACTACCTGCCACGAACTGGCGATTCCGGCATATCGTCACAT
GGCGTTGCTGAACGACCTGGTTTCTTGGGAGAAAGAACGTGCATCTAGCATCGC
GCTGGGTAAAGACTACTGCATCAACTTCATCTTCGTTGCTATGGAAGAATCTGGT
ATCAGCGAAGACGAAGCGAAAGAACGTTGCCGTGAAGAAATCAAACTGGCGAC
CGTTGACTACCTGCGTGTGTTCGACGAAGCGAAAGACCGTATCGACCTGTCTCAC
GACACTATGCTGTACCTGGAAAGCCTGCTGTACTCCATGTCTGGTAACGTTGTTT
GGGGTCTGCAGTCTCCACGTTACTACACTGACGCGAAATTCAGCCAGCGTCAGCT
GGACTGGATCAAGAACGGTTTGCCGCTGGAAGTGCGTCTGGAAGATCGTGTGTT
CGGTCTGAGTCCGTCTGAAGACCGTGTTACTCACCAGGCAGTAATCGAGAATGG
CCTGCCAGAATCTGGTCTGGGTAAGAACGGTAACTCTTCCAACGGTGTTGACGTT
AACAAAGCGCTGCTGTCTGCTGTACTGCACGAACACCTGAAAGGTCACGCGGTA
TTCAAGATGTCTGATCACGAAGTGAAGGTTAAAGCTTCTAACGGTCGTAGCCTGG
ACACTAAAGTTCTGCAGGCGCCATACGAATACATCACCGGTCTGCCGTCTAAACG
TCTGCGTGAACAGGCGATCGATGCTATGAACGTTTGGTTCCGTGTTCCAGCGGAG
AAACTGGACCTGATCAAATCCATCACCACCATCTTGCACAACGCGTCTCTGATGC
TGGACGACGTTGAAGACGGTTCTGAACTGCGTCGTGGTAATCCATCTACTCACAC
CATCTTCGGTCTTAGCCAGACCATCAACTCTGCGAACTACCAGCTGGTTCGTGCA
CTGGAACGCGTTCAGAAACTGGAAGACTCTGAAAGCTTGCTGGTGTTCACTGAA
GAACTGCGTAACCTGTACATCGGTCAGTCTATGGACCTGTACTGGACTGGTAACC
TGATCTGCCCGACCATGAACGAATACTTCCACATGGTTGAATGCAAGACCGGTG
GTCTGTTCCGTCTCTTTACCCGTCTGATGTCTCTGCACTCCACCTCTGCAGTTAAA
GTTGATCCGACCACTCTGTCCACTCGTCTGGGTATCTACTTCCAGACTCGTGACG
ACTACAAGAACCTGGTATCTACTGAGTACACCAAACAGAAAGGCTACTGTGAAG
ATCTGGAAGAAGGCAAATTCTCTCTGCCGCTGATCCACCTGATCCAGGCAATGCC
AGATAACCACGTTCTGCGTAACATTCTGACTCAGTGGCGTGTTACTCGTAAAGTA
ACTCTGGCGCAGAAACAGGTTGTACTCGGTCTGATGGAGAAGTCCGGTAGCCTG

AAATTCACTCGTGAAACTCTGGCTAGCCTGTACTCTGGCCTGGAAAAAAGCTTCA
CCGAACTGGAAGAGAAATTCGGCACTGAGAACTTCCAGCTGAAACTGATTCTGC
AGTTCTTGCGTACTGAA

SUPPORTING FIGURES

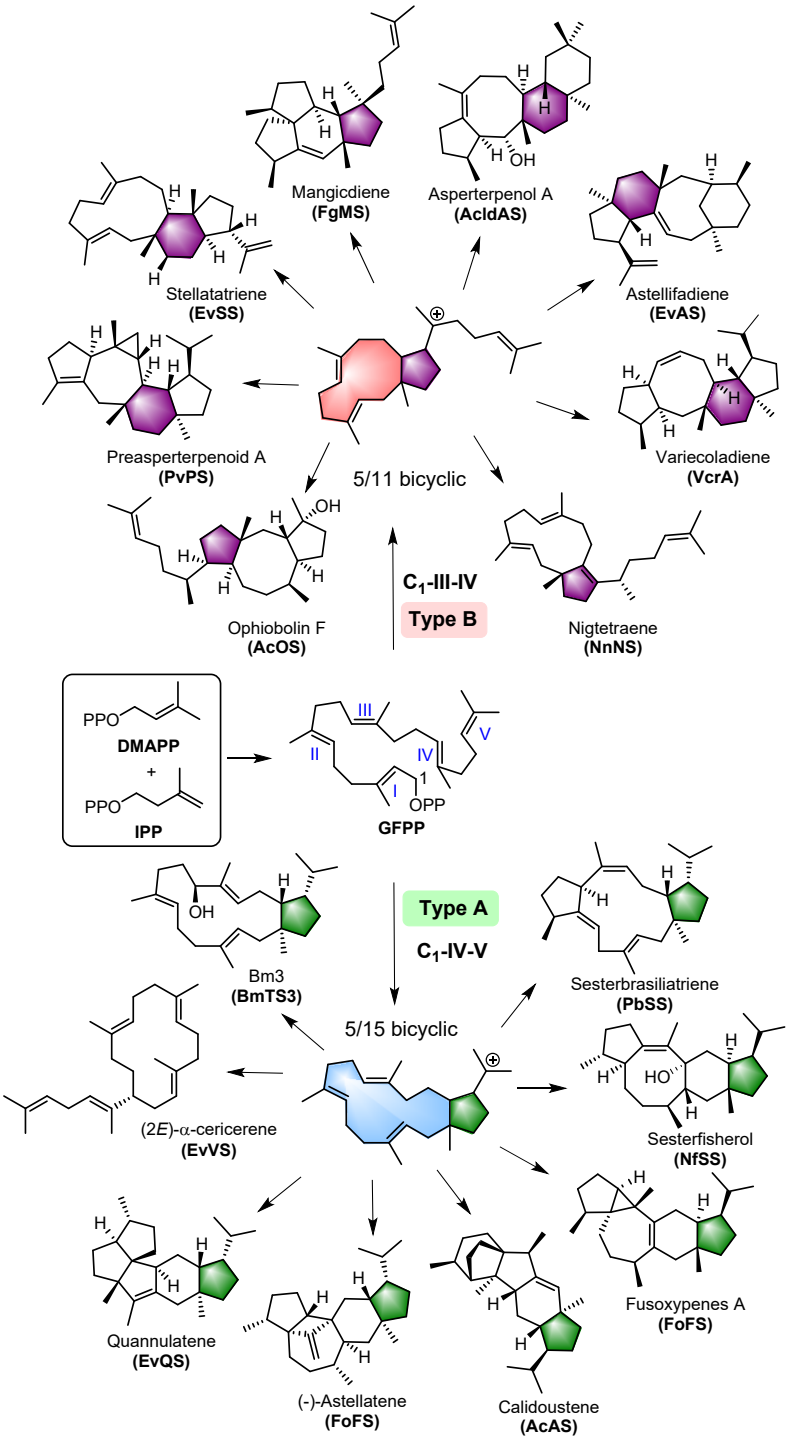

Figure S1. Schematic diagram of the cyclization patterns correlated with representative sesterterpenes catalyzed by bifunctional terpene synthases (BFTPSs) from fungi. Their cyclization patterns were correlated with the initial cyclization mode of a polyprenyl diphosphate, defined as Type A and Type B. Following pyrophosphate dissociation, the carbocation at C1 selectively engages with the IV and V double bonds in Type A, while targeting the III and IV double bonds in Type B.[16]

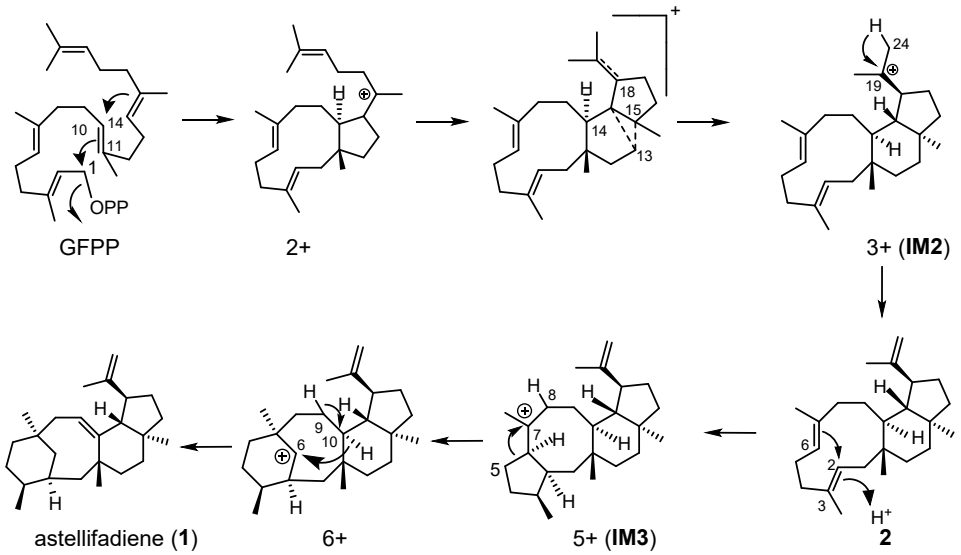

Figure S2. Proposed reaction mechanism for the generation of **1**.[1]

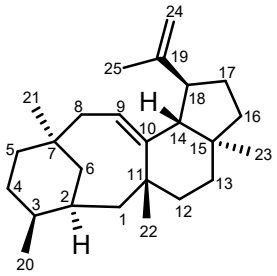

astellifadiene (**1**)

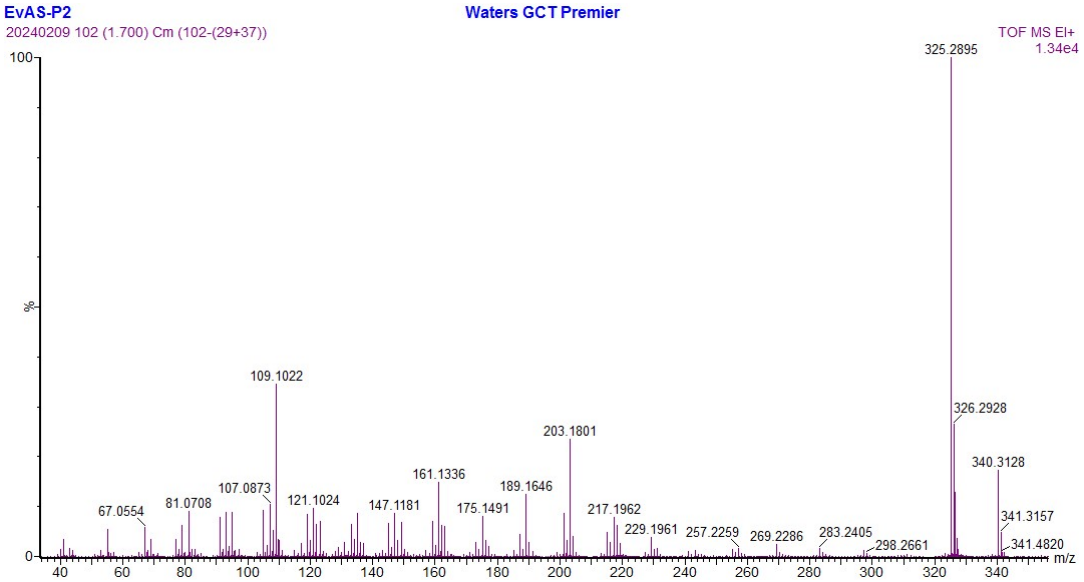

Figure S3. HR-EI-MS spectrum of **1**.

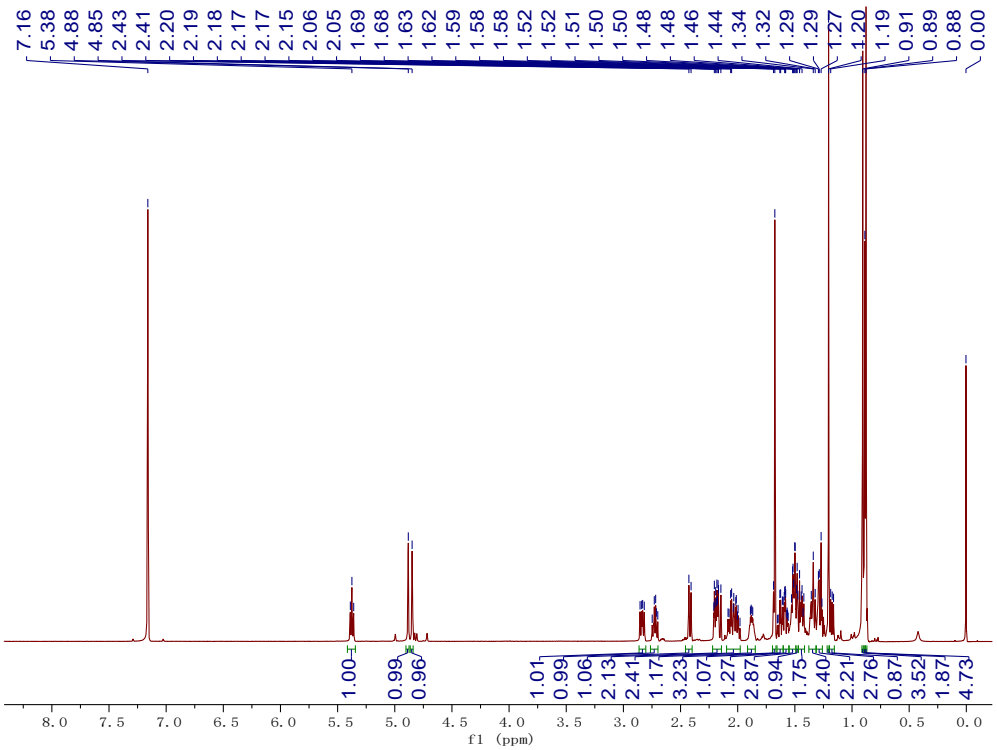

Figure S4. ^{1}H NMR (600 MHz, C_6D_6) spectrum of **1**.

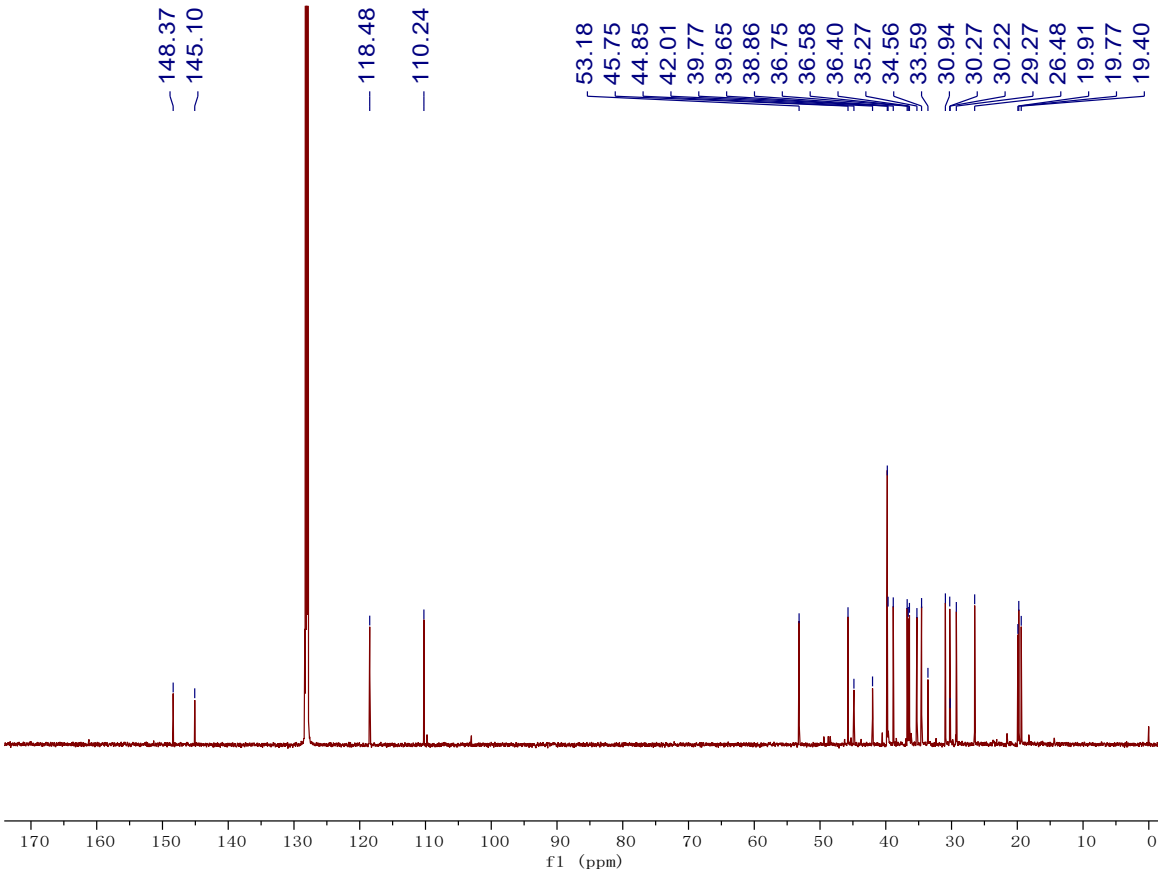

Figure S5. ^{13}C NMR (150 MHz, C_6D_6) spectrum of **1**.

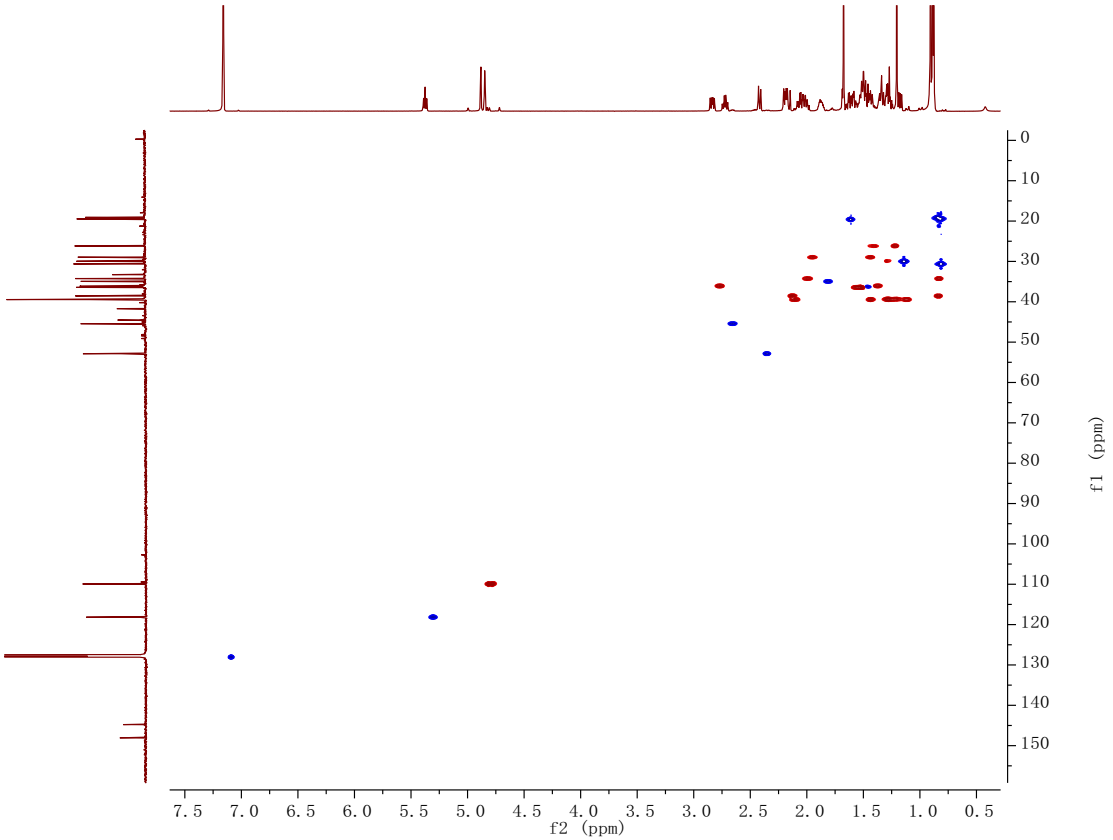

Figure S6. HSQC NMR (600 MHz, C_6D_6) spectrum of **1**.

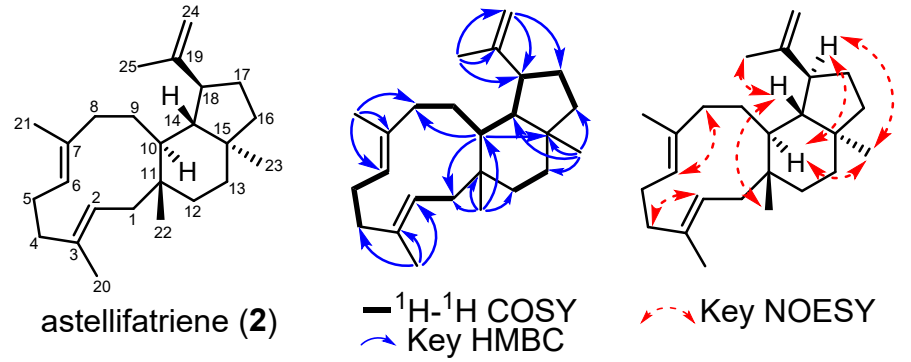

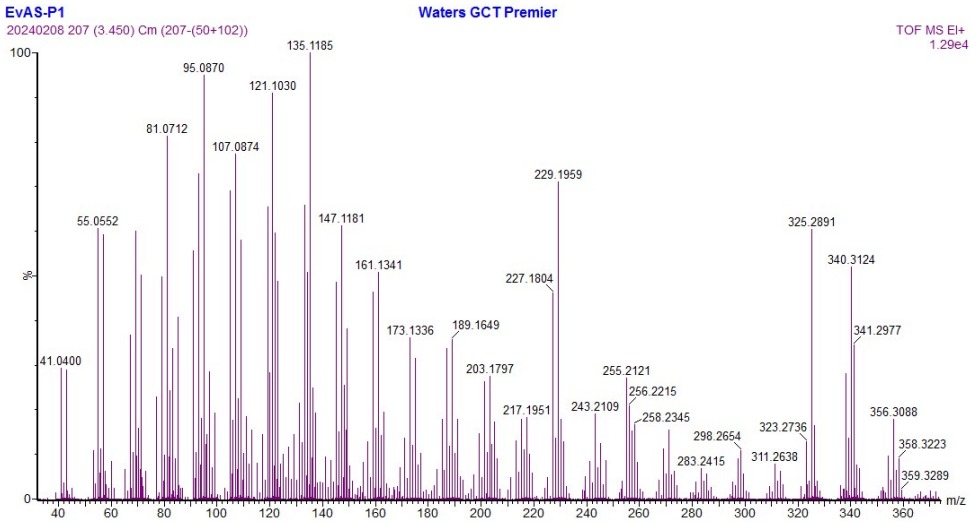

Figure S7. HR-EI-MS spectrum of **2**.

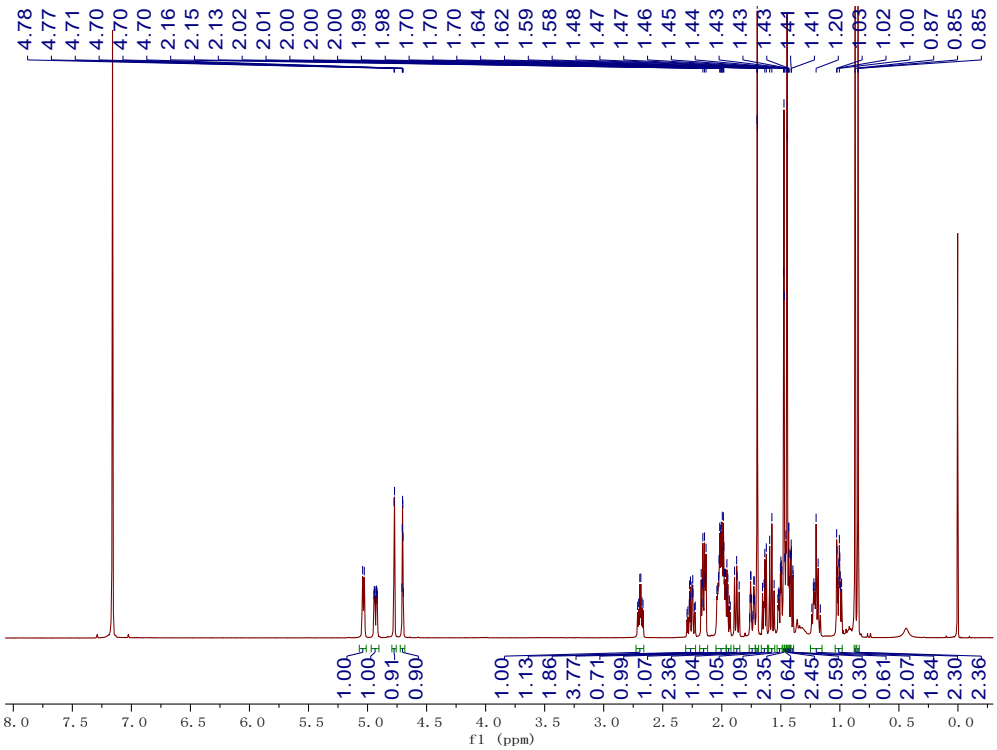

Figure S8. ^{1}H NMR (600 MHz, C_6D_6) spectrum of **2**.

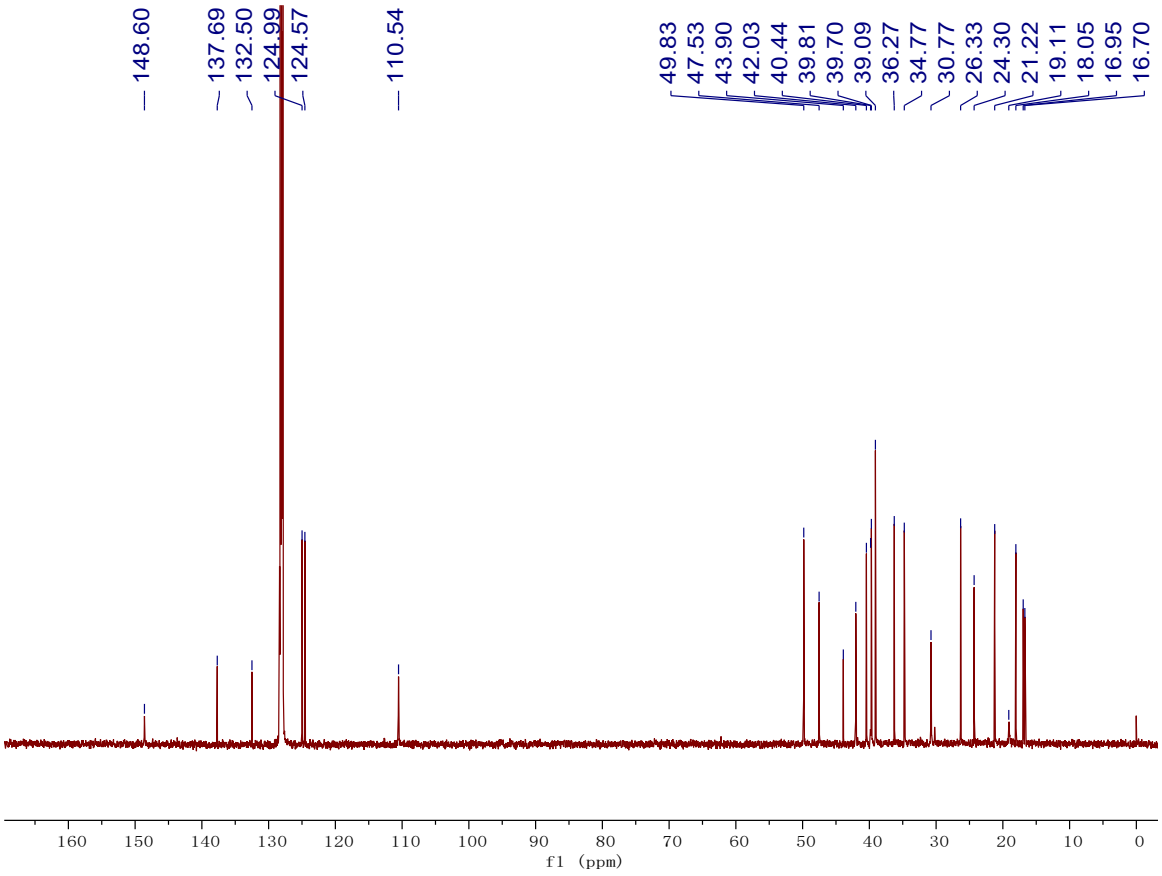

Figure S9. ^{13}C NMR (150 MHz, C_6D_6) spectrum of **2**.

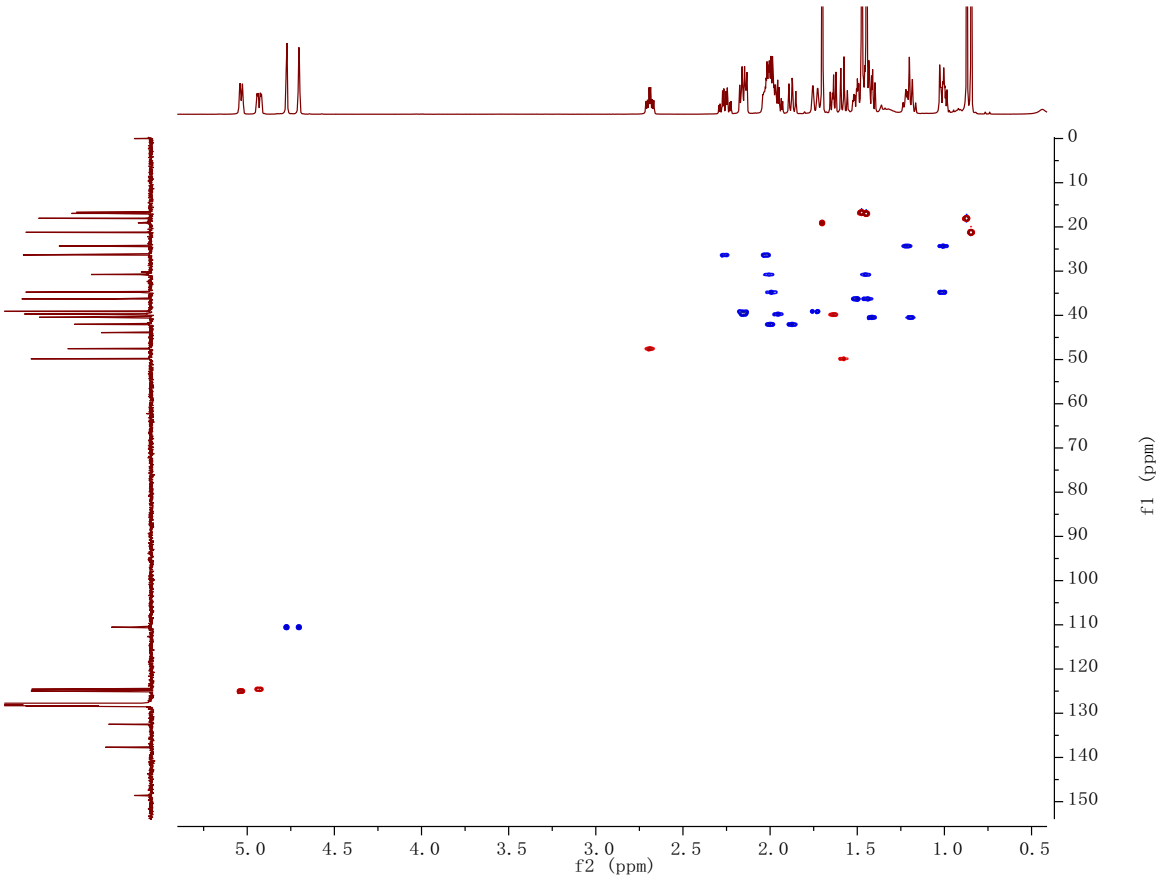

Figure S10. HSQC NMR (600 MHz, C_6D_6) spectrum of **2**.

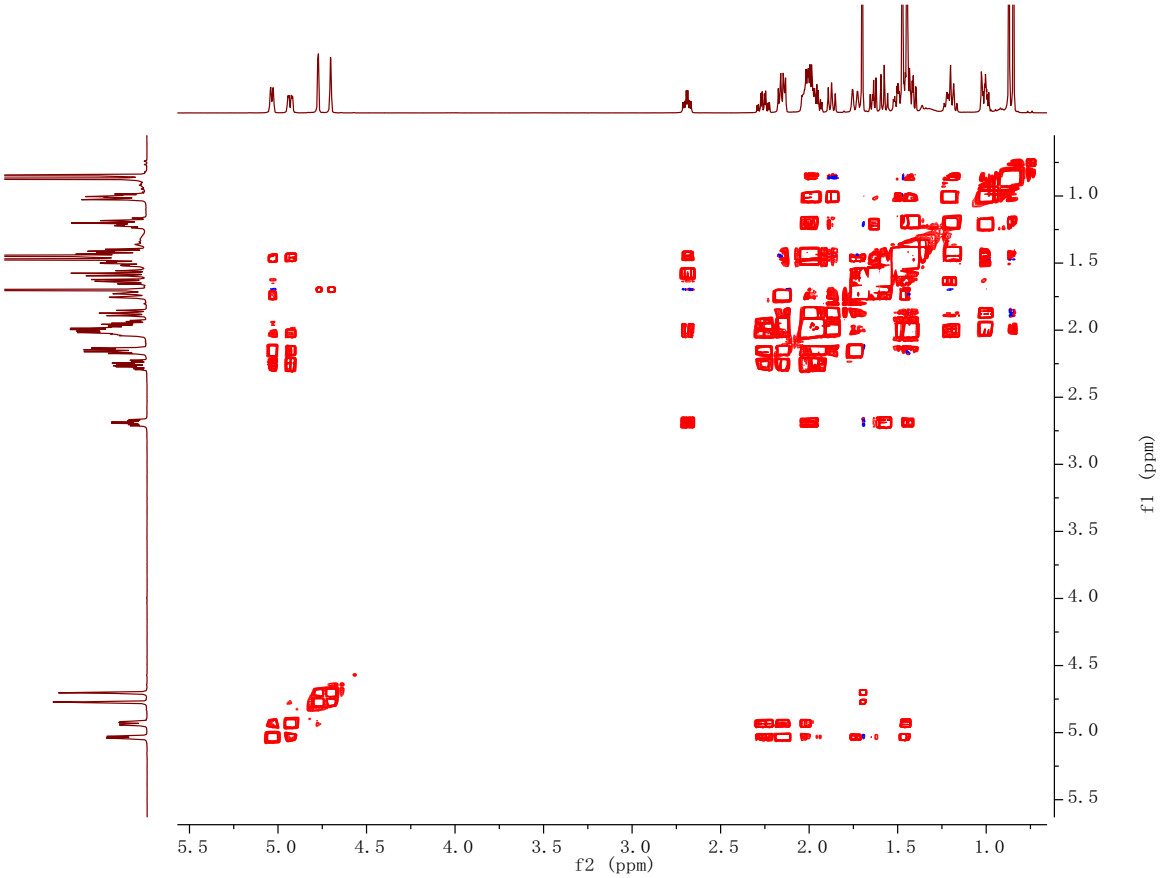

Figure S11. ^1H–^1H COSY NMR (600 MHz, C_6D_6) spectrum of **2**.

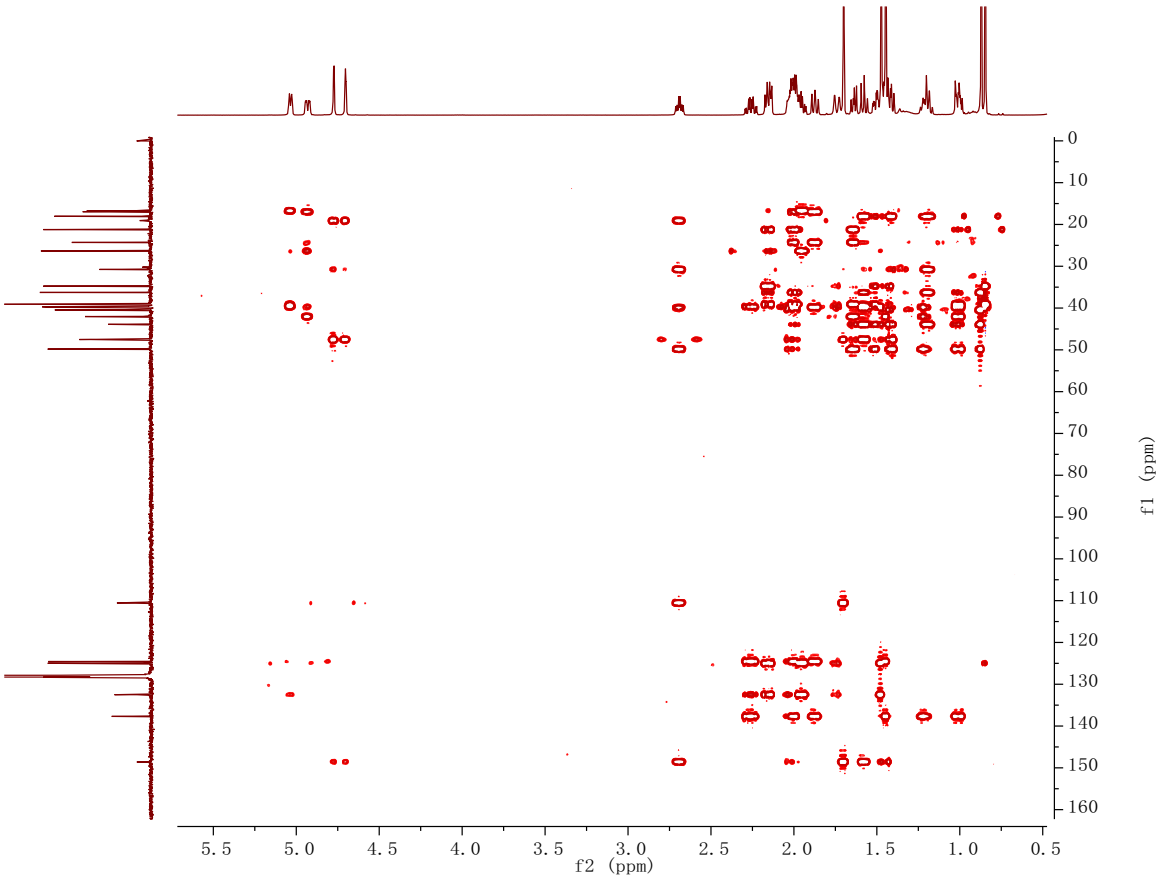

Figure S12. HMBC NMR (600 MHz, C_6D_6) spectrum of **2**.

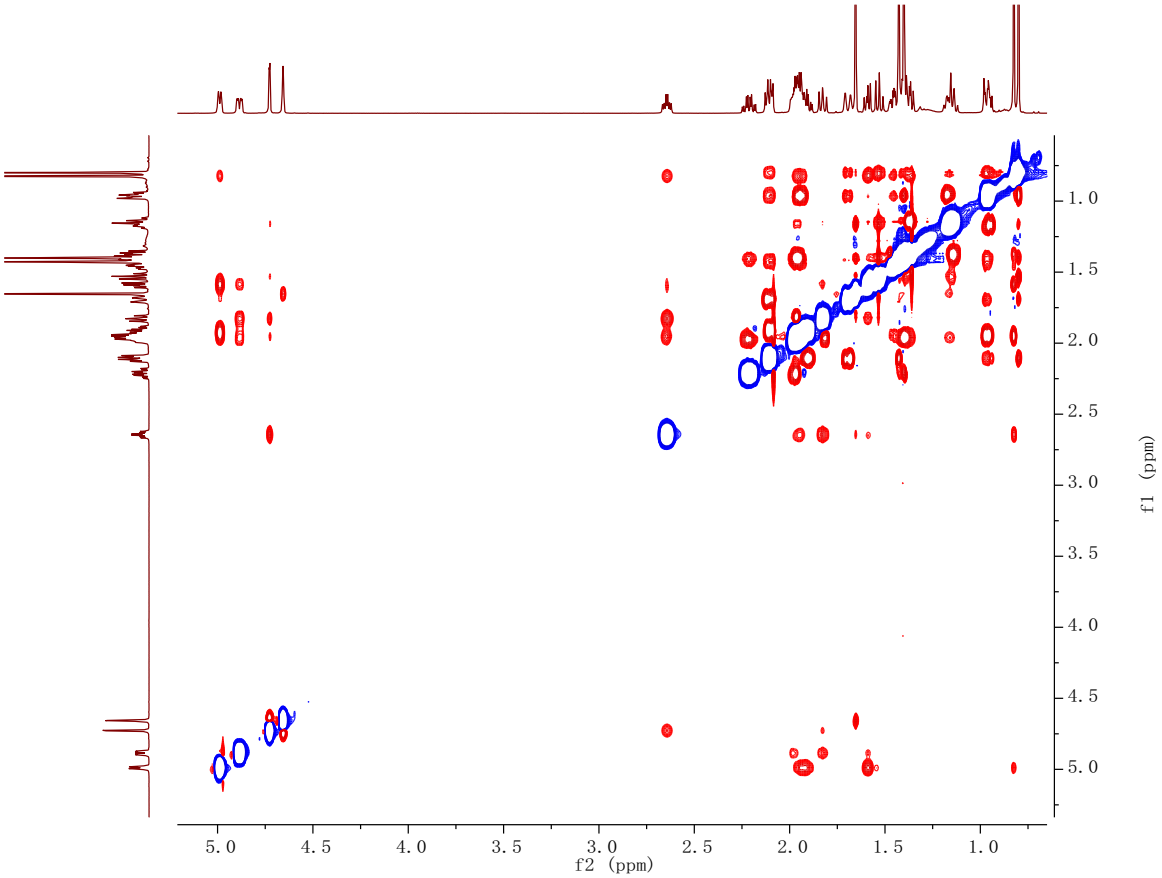

Figure S13. NOESY NMR (600 MHz, C_6D_6) spectrum of **2**.

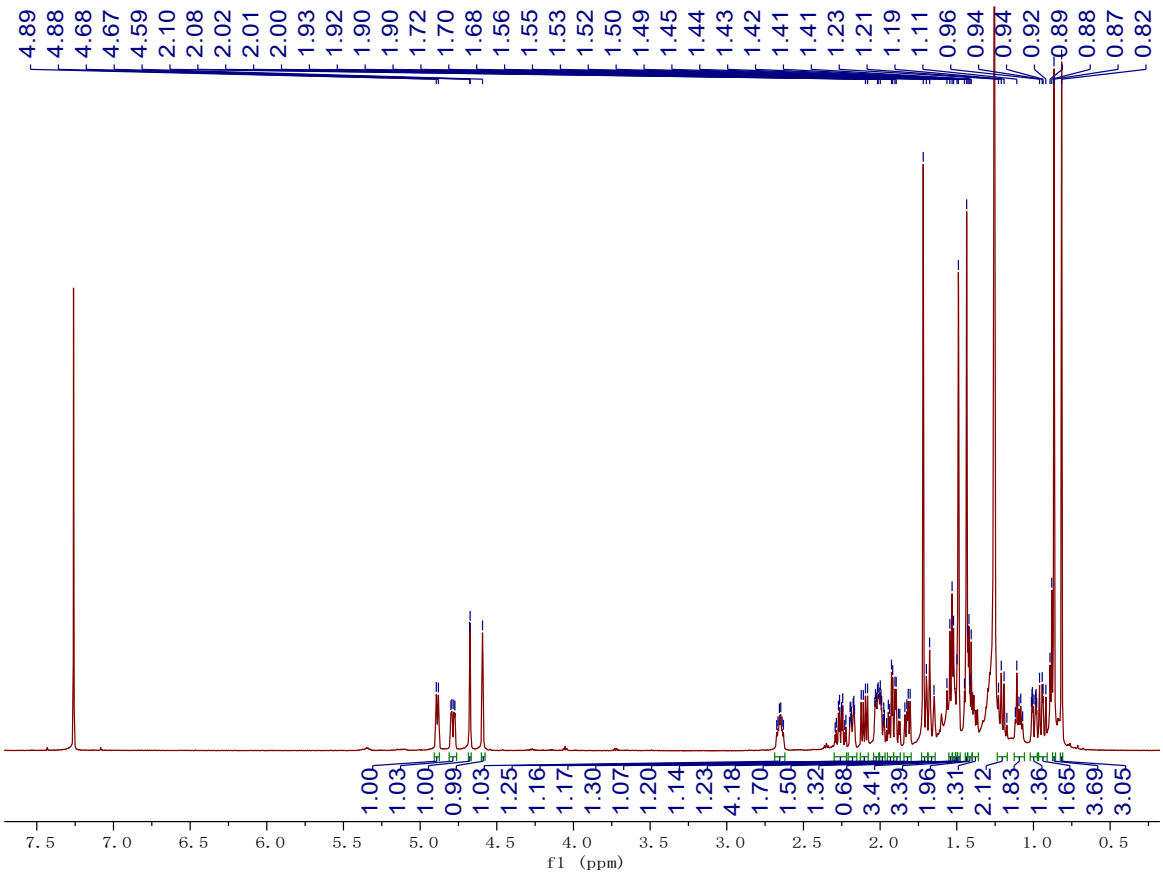

Figure S14. ^{1}H NMR (600 MHz, $CDCl_3$) spectrum of **2**.

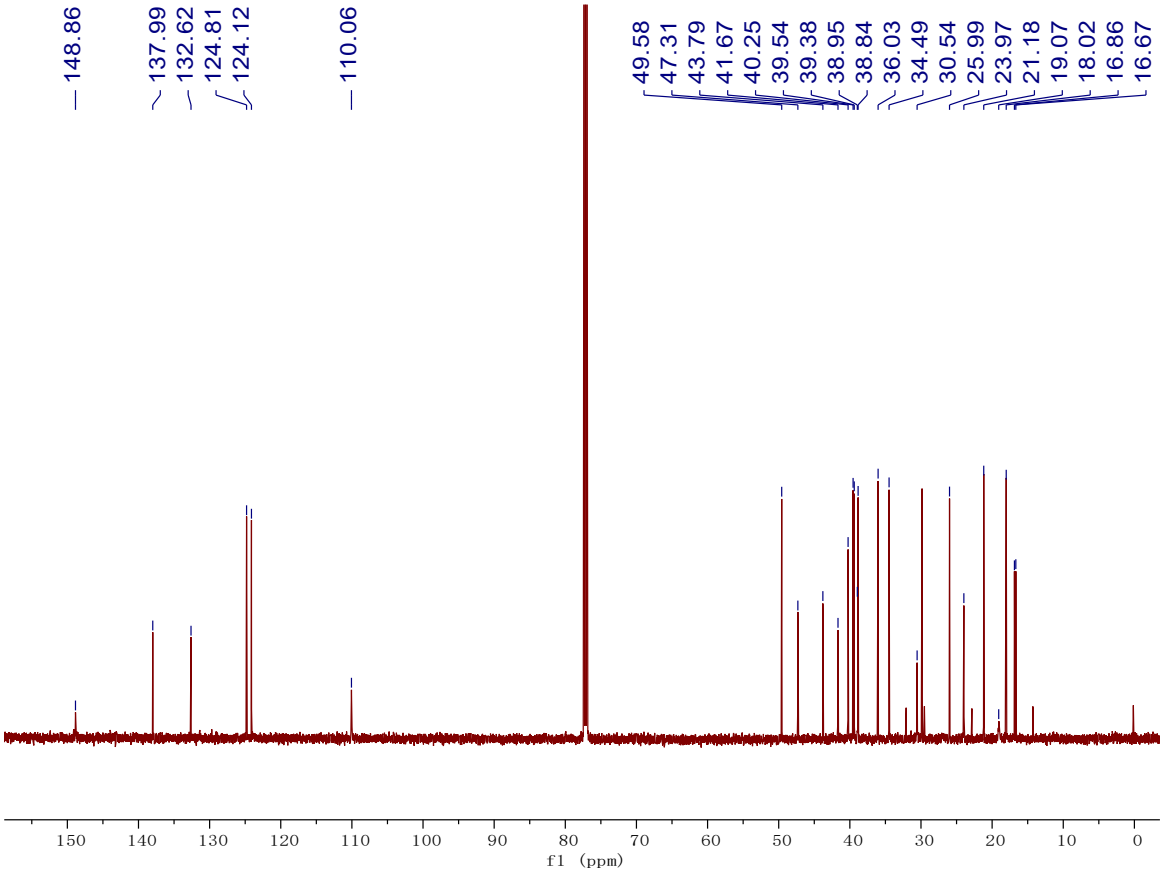

Figure S15. ^{13}C NMR (150 MHz, $CDCl_3$) spectrum of **2**.

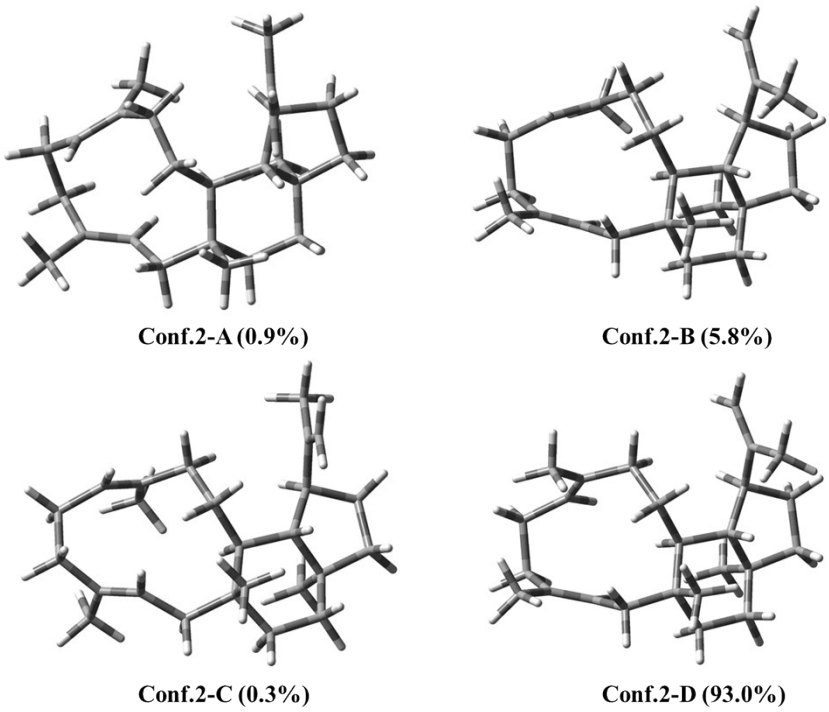

Figure S16. The optimized lowest energy conformers for (2*E*,6*E*,10*S*,11*R*,14*S*,15*S*,18*S*)-**2** at the B3LYP/6-31G(d).

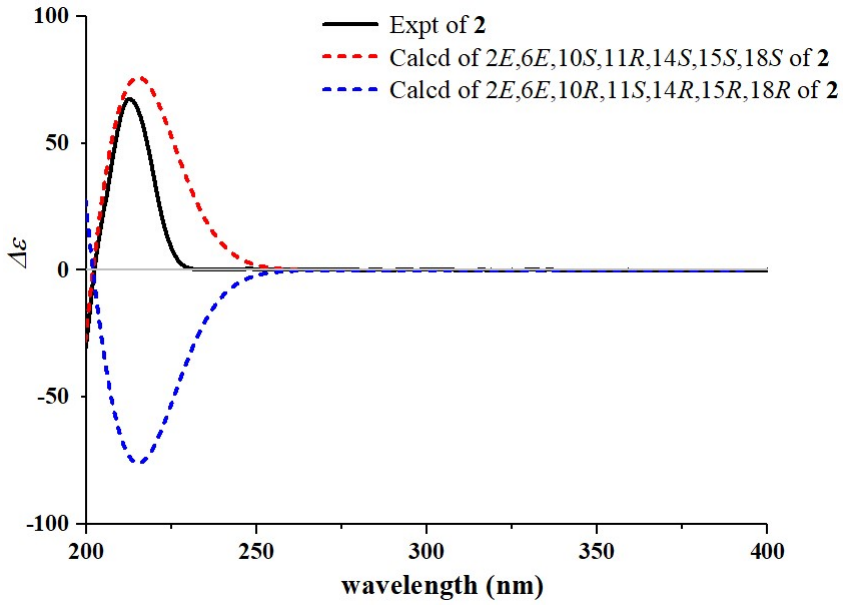

Figure S17. Experimental and calculated (B3LYP/6-31G(d,p)) ECD spectra of **2**.

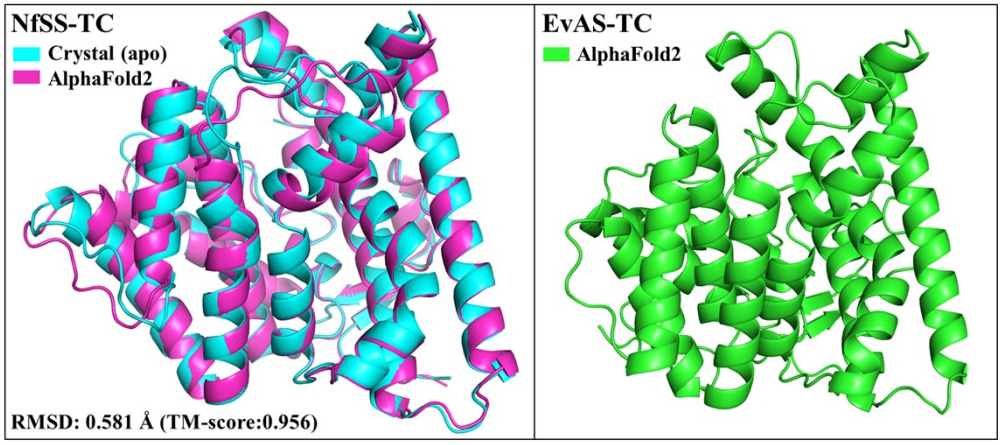

Figure S18. Protein models of TC domains of NfSS and EvAS predicted using AlphaFold2. The predicted NfSS-TC is similar with the reported crystal structure (8yla) (TM-score 0.956). The RMSD calculations of the NfSS-TC crystal structure (PDB entry 8yla) was superimposed on the heavy chain of the AlphaFold model of NfSS-TC via the Cα atoms of 250 residues.

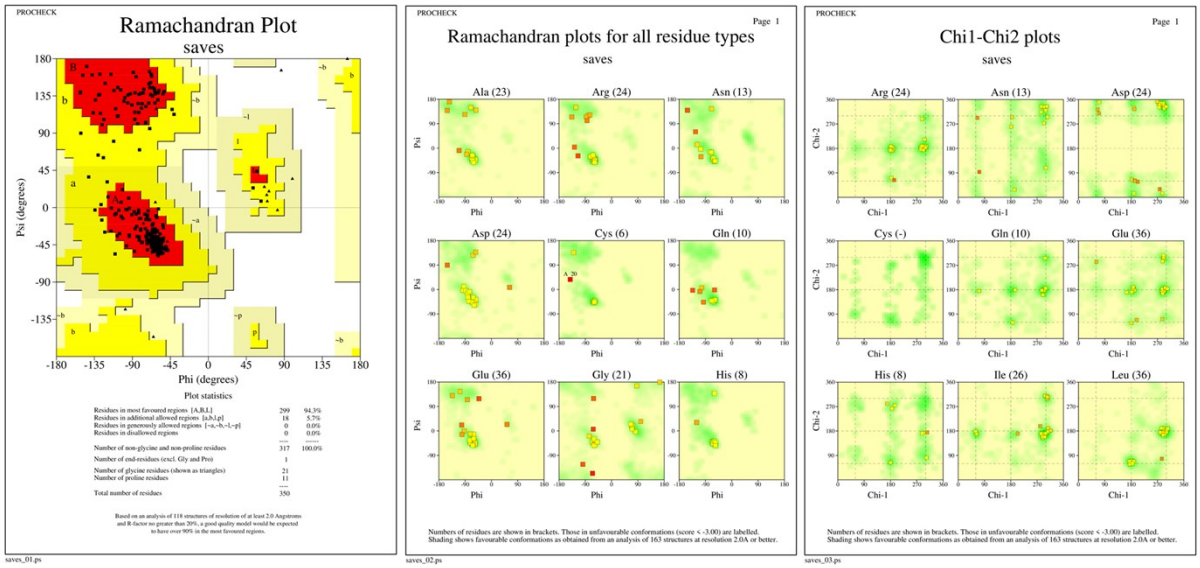

Figure S19. The PROCHECK results of EvAS-TC model indicate the good quality of the model predicted using AlphaFold2.

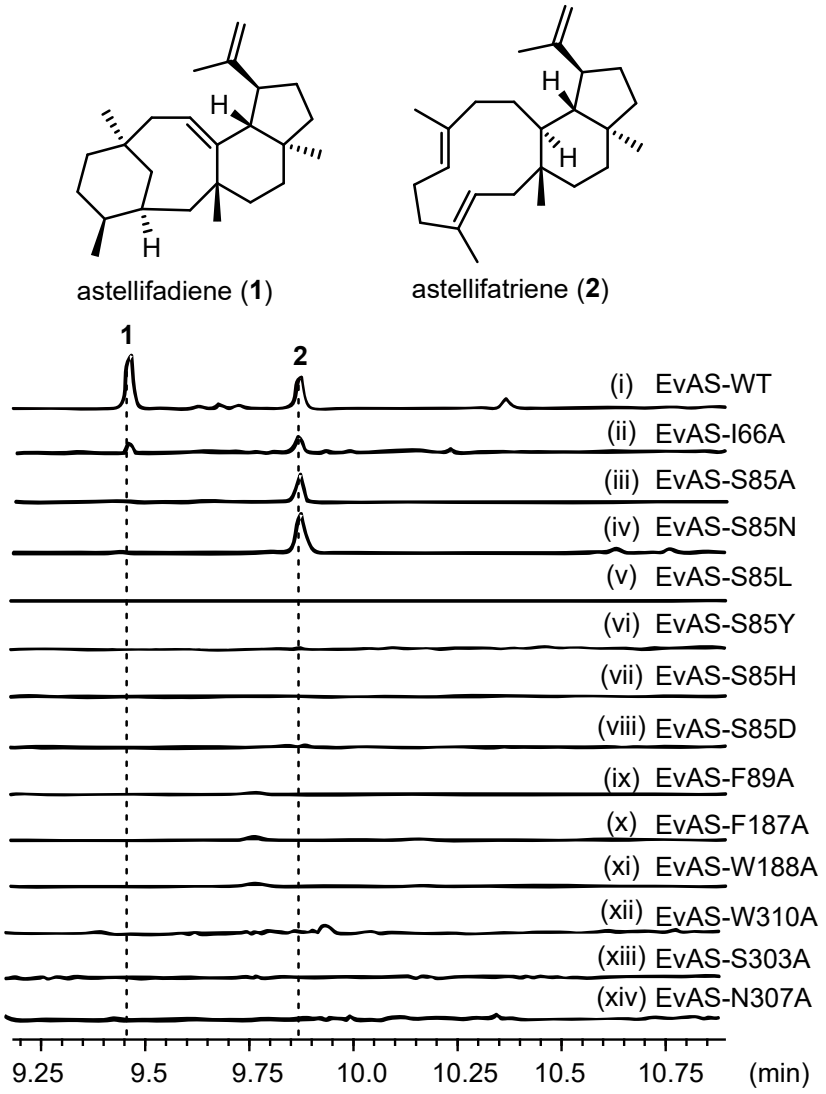

Figure S20. The structure of isolated compounds **1**–**2** and GC-MS profiles of crude extracts obtained from EvAS-WT, and its variants.

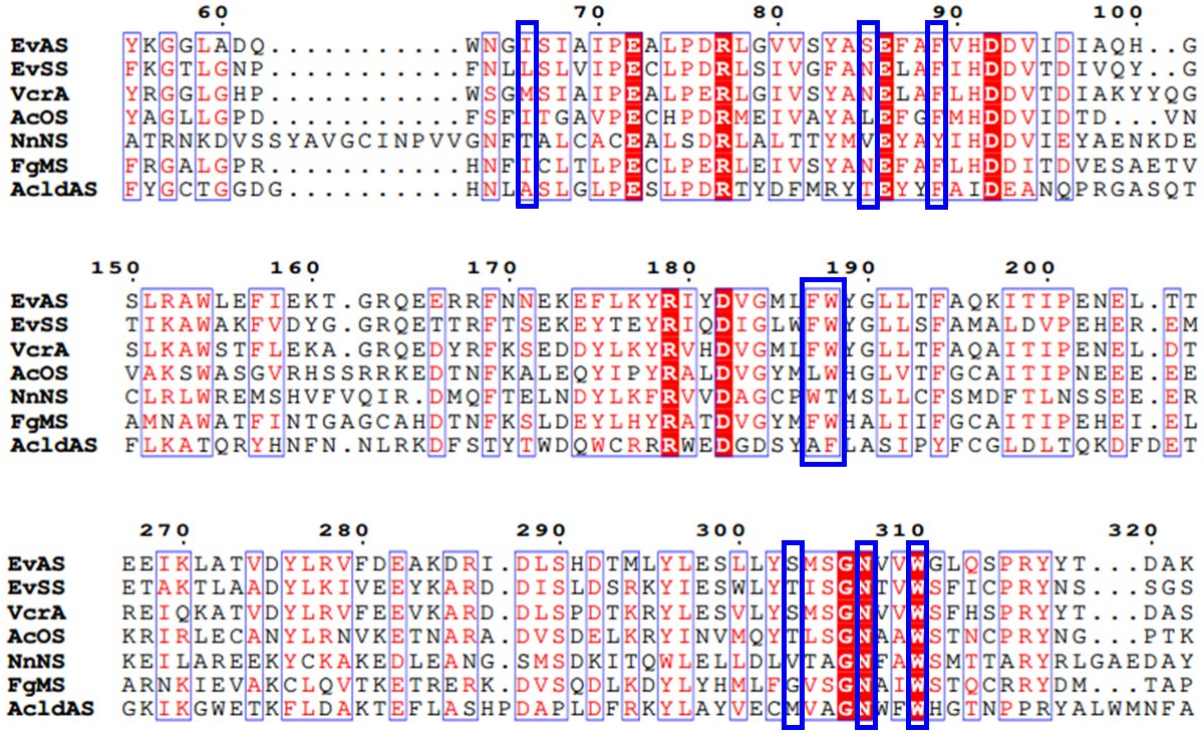

Figure S21. Amino acid sequence alignments of Type B BFTPSs.

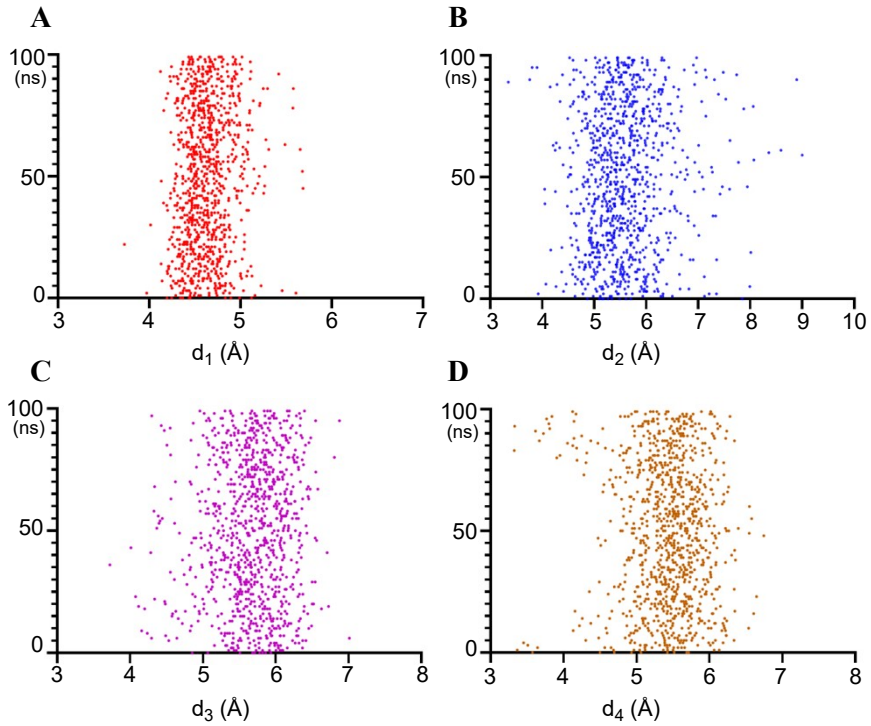

Figure S22. Scatter diagrams of the conformations of the EvAS-WT/**IM2** and EvAS-WT/**2** complexes. Scatter plots of the conformations of the EvAS-WT/**IM2** complex are presented, showing the distances from C19 to W188 (A, d_1) and from H24 to S303 (B, d_2). And scatter plots display the distances from C3 to the S85 carbonyl oxygen (C, d_3) and from C3 to the S85 hydroxyl oxygen (D, d_4) for all conformations of the EvAS-WT/**2** complex.

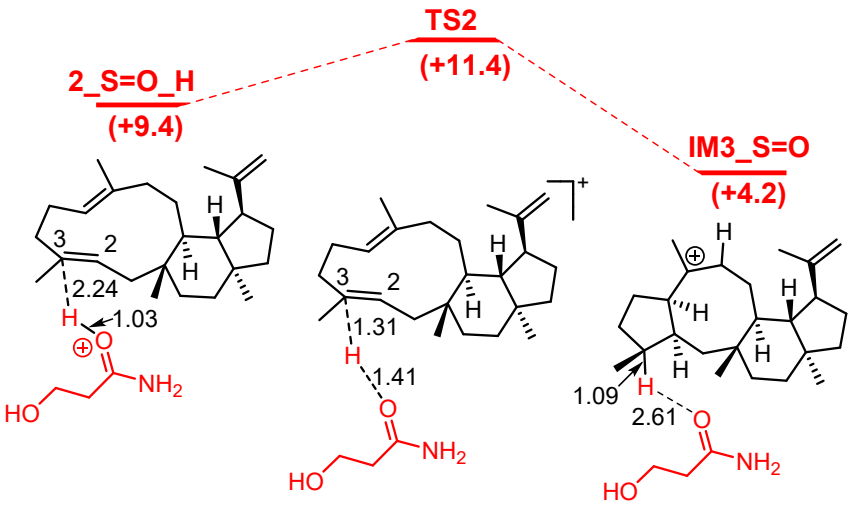

Figure S23. The Gibbs free energy profiles (in kcal/mol) for reprotonation sequence mediated by carbonyl oxygen of serine, progressing from state **2** to **IM3**, computed using the mPW1PW91/6-311+G(d,p)//B3LYP/6-31G(d) method relative to **2_S-O_H** are shown in red.[17-20]

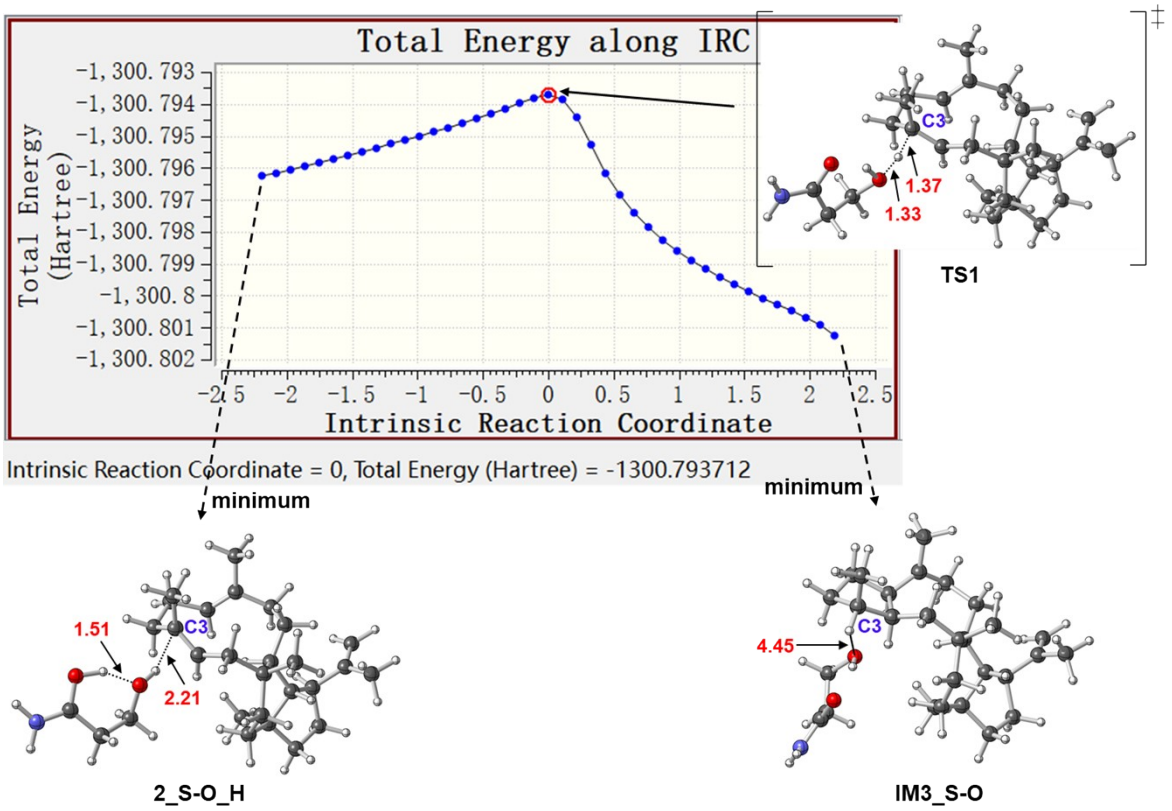

Figure S24. Conversion of **2_S-O_H** to **IM3_S-O** from IRC calculations (The red numbers denote interatomic distances (Å), while the blue numbers signify the carbon atom's sequential order).

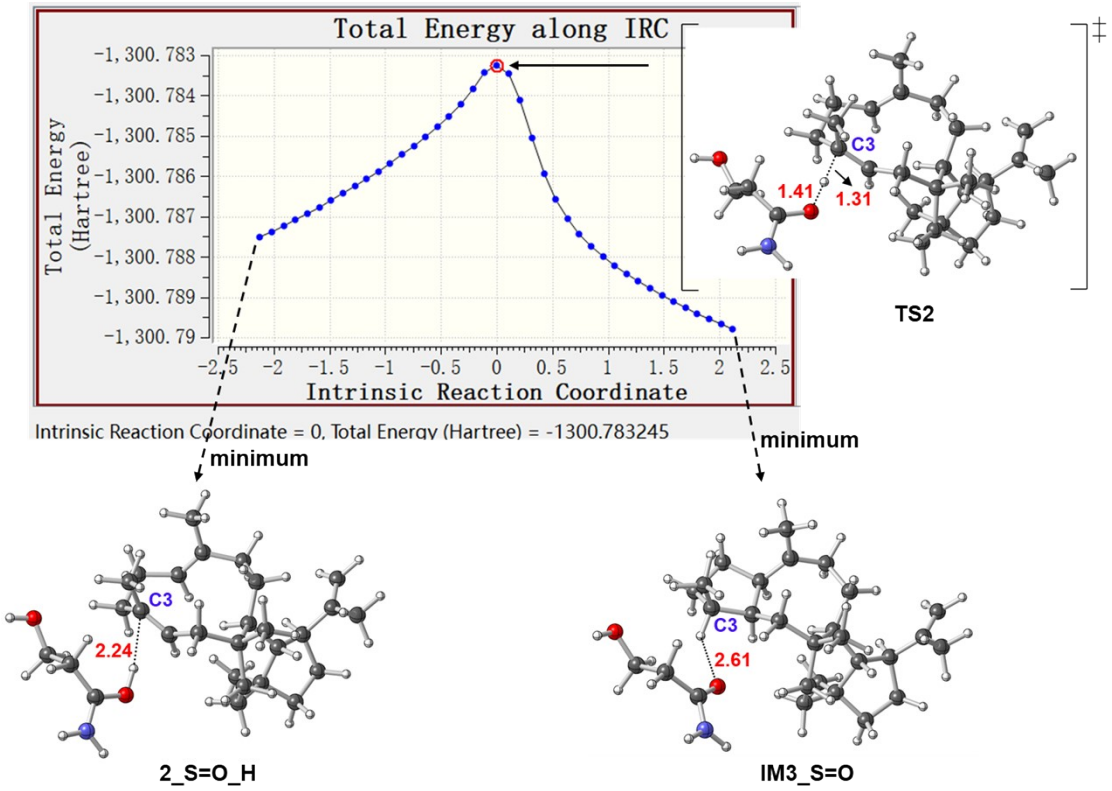

Figure S25. Conversion of **2_S=O_H** to **IM3_S=O** from IRC calculations (The red numbers denote interatomic distances (Å), while the blue numbers signify the carbon atom's sequential order).

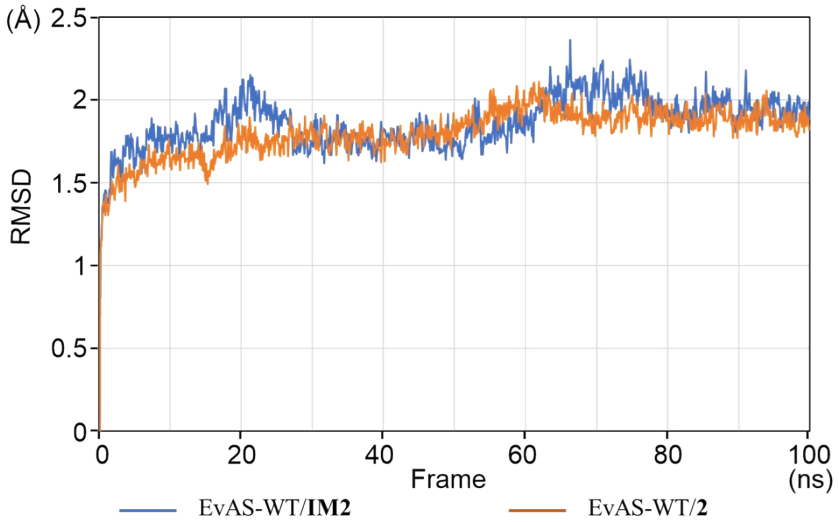

Figure S26. The RMSD profiles of the protein backbones of EvAS-WT/**IM2**, and EvAS-WT/**2**, during 100 ns (x 2) molecular dynamics simulations.

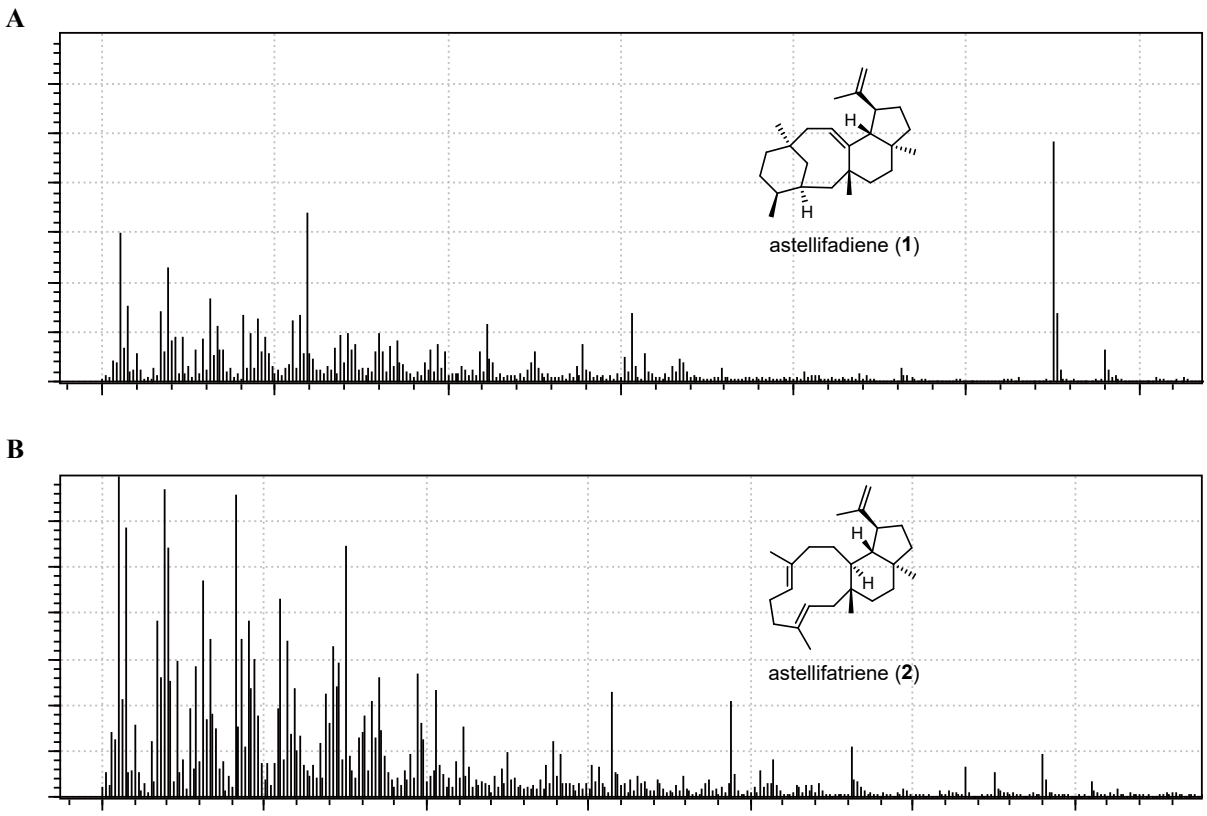

Figure S27. Mass spectra of (A) astellifadiene (**1**) and (B) astellifatriene (**2**) from the transformants.

SUPPORTING TABLES

Table S1. The bifunctional terpene synthases characterized from fungi and their products.

No.	Protein	Accession	Species	Products	Ref, year
1	AcOS	A1C8C3.1	*Aspergillus clavatus*	Ophiobolin F, Ophiobolane 1, Ophiobolane 2, Clavaphyllen	[21], 2013
2	Au8003	QIH97826.1	*Aspergillus ustus*	Ophiobolin F	[22], 2016
3	BmOS	MW798226	*Bipolaris maydis*	Ophiobolin F	[23], 2021
4	AuOS	MW798208	*Aspergillus ustus*	Ophiobolin F	[23], 2021
5	PfVS	MW798216	*Pestalotiopsis fici*	Clavaphyllene, Variculatriene A, *β*-Geranylfarnesene	[23], 2021
6	EvVS	LC063849	*Emericella variecolor*	Variediene, (2*E*)-*α*-cericerene	[24], 2015
7	EvAS	LC113889	*Emericella variecolor NBRC 32302*	Astellifadiene	[1], 2016
8	BmTS1	EMD84919	*Bipolaris maydisATCC48331*	Bm1	[25], 2017
9	BmTS2	EMD93209	*Bipolaris maydisATCC48331*	Bm2	[25], 2017
10	BmTS3	EMD93704	*Bipolaris maydisATCC48331*	Bm3	[25], 2017
11	CfBS	MW798209	*Colletotrichum fioriniae*	Bm3	[23], 2021
12	MpBS	MW798229	*Macrophomina phaseolina*	Bm3	[23], 2021
13	PbTS1	LC274619	*Phoma betae PS-13*	Pb1	[25], 2017
14	BtcAco	N4V6D4.1	*Colletotrichum orbulare*	Pb1	[26], 2018
15	ChPS	MW798213	*Colletotrichum higginsianum*	Pb1	[23], 2021
16	CsPS	MW798219	Colletotrichum siamense	Pb1	[23], 2021
17	CoFS	MW798210	*Colletotrichum orbiculare*	Pb1, Fusaproliferene	[23], 2021
18	CiGS	MW798200	*Colletotrichum incanum*	Pb1, *β*-Geranylfarnesene	[23], 2021
19	FgMS	AQY56777	*Fusarium graminearum*	Mangicdien, Variecoltetraene	[27], 2017
20	NfSS	EAW16201	*Neosartorya fischeri*	Sesterfisherol	[28], 2015
21	AaSS	MW798204	*Alternaria alternata*	Sesterfisherol	[23], 2021
22	CiSS	MW798201	*Colletotrichum incanum*	Sesterorbiculene	[23], 2021
23	CoSS	MW798211	*Colletotrichum orbiculare*	Sesterorbiculene	[23], 2021
24	CgSS	MW798218	*Colletotrichum gloeosporioides*	Sesterorbiculene	[23], 2021
25	ChVS	MW798212	*Colletotrichum higginsianum*	(-)-Variculatriene B	[23], 2021

26	PoVS	MW798215	*Pyricularia oryzae*	(-)-Variculatriene B	[23], 2021
27	LmVS	MW798221	*Lophiostoma macrostomum*	(-)-Variculatriene B	[23], 2021
28	CsVS	MW798223	*Colletotrichum sublineola*	(-)-Variculatriene B	[23], 2021
29	PoVS	MW798227	*Pyricularia oryzae*	(-)-Variculatriene B	[23], 2021
30	TtPS	MW798214	*Thermothielavioides terrestris*	Preasperterpenoid A	[23], 2021
31	PvPS	LC228602	*Penicillium verruculosum*	Preasperterpenoid A	[29], 2017
32	AsTC	MK140602	*Talaromyces wortmannii*	Preasperterpenoid A	[30], 2019
33	TvPS	MW798225	*Talaromyces verruculosus*	Preasperterpenoid A	[23], 2021
34	PaSS	MW798222	*Penicillium arizonense*	Sesterbrasiliatriene	[23], 2021
35	PbSS	LC228601	*Penicillium brasilianum*	Sesterbrasiliatriene	[29], 2017
36	ChBS	MW798232	*Colletotrichum higginsianum*	Brassiteraene A, Brassiteraene B	[23], 2021
37	ZbSS	MW798202	*Zymoseptoria brevis*	Sesterevisene	[23], 2021
38	AnGS	MW798203	*Aspergillus niger*	Geranylfarnesol	[23], 2021
39	PgGS	MW798206	*Penicillium griseofulvum*	Geranylfarnesol	[23], 2021
40	PgFS	MW798217	*Pyricularia grisea*	Geranylfarnesol	[23], 2021
41	TaGS	MW798220	*Thielavia arenaria*	Geranylfarnesol	[23], 2021
42	AaGS	MW798231	*Aspergillus aculeatus*	Geranylfarnesol	[23], 2021
43	CsSS	MW685620	*Cytospora schulzeri 12,565*	Schultriene	[31], 2022
44	NnNS	MW685621	*Nectria nigrescens 12,199*	Nigtetraene	[31], 2022
45	EvSS	LC073704	*Emericella variecolor*	Stellata-2,6,19-triene	[32], 2015
46	EvQS	LC155210	*Emericella variecolor*	Quannulatene	[33], 2016
47	AcldAS	CEL06489.1	*Aspergillus calidoustus CBS121601*	Asperterpenol A	[34], 2020
48	AuAS	MW387950	*Aspergillus ustus 094102*	Aspergildiene A, Aspergilols A−D	[35], 2021
49	FoFS	MW446505	*Fusarium oxysporum*	Fusoxypenes A-C, (-)-astellatene	[36], 2021
50	AtAS (StTA)	ATEG_03568 (KX449366)	*Aspergillus terreus*	Preaspterpenacid I	[36, 37], 2021, 2017
51	BsPS	NA	*Bipolaris sorokiniana*	Preterpestacin I,	[38], 2021
52	AcAS	NA	*Aspergillus calidoustus*	Aspergiltriene, Aspergildienes A–D, calidoustene	[39], 2022
53	AaTPS1	XP_018386201	*Alternaria alternata MB-30*	sesteraltererol	[40], 2023
54	AaTPS2	XP_018380014	*Alternaria alternata MB-30*	preterpestacin I	[40], 2023
55	PsTA	NA	*Penicillium herquei TJ403-A1*	Penisentene	[41], 2022
56	VrcA	XP_020054773.1	*E. variecolor NBRC 32302*	Variecoladiene	[42], 2024
57	EmES	WWS34622.1	*Emericellasp*	Emerindanol A and B	[43], 2024

58	PaFS	A2PZA5.1	*Phomopsis amygdali*	Fusicocca-2,10(14)-diene	[44], 2007
59	AbFS	AB465604	*Alternaria brassicicola*	Fusicocca 2,10(14)-diene	[45], 2008
60	CgDS	P9WEV7.1	*Colletotrichum gloeosporioides ES026*	(1*R*)-*δ*-Araneosene (5*R*,12*R*,14*S*)-dolasta-1(15),8-diene	[46], 2018
61	CpPS	NA	*Clitopilus passeckerianus*	Premutilin	[47], 2018
62	PaPS	NA	*Phomopsis amygdali*	Phomopsene	[48], 2009
63	PcCS	LC411963	*Penicillium chrysogenum*	Penichrysol	[49], 2018
64	PrDS	W6QAE7.1	*Penicillium roqueforti*	Penichrysol	[50], 2018
65	DvVS	ON911568	*Didymosphaeria variabile 17020*	Variediene, Neoflexibilene, Neovariediene	[51], 2022
66	TndC	NA	*Aspergillus flavipes*	Talarodiene	[52], 2022
67	TlnA	NA	*Talaromyces stipitatus*	Talarodiene, Talarodiene B.	[53], 2024
68	AfAS	BK065787	*Aspergillus fumigatiaffinis*	Asperfumene	[54], 2024
69	MpMS	EKG20455.1	*Macrophomina phaseolina*	Macrophomene	[55], 2022
70	TvTS	KUL85185.1	*Talaromyces verruculosus*	Talaropentaene	[55], 2022
71	CgCS	A0A8H4CUY8.1	*Colletotrichum gloeosporioides*	Colleterpenol	[55], 2022

NA indicates not available.

Table S2. Comparison of ^{1}H (600 MHz) and ^{13}C (150 MHz) NMR (in benzene-d_6) data of **1** to those of astellifadiene (500 MHz, in benzene-d_6) in the literature.[1]

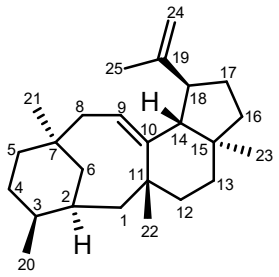

astellifadiene (**1**)

Pos.	δ_H mult (J in Hz), **1**	δ_C, **1**	δ_H mult (J in Hz), astellifadiene	δ_C, astellifadiene
1	1.18, dd (15.3, 6.7); 2.17, m	39.7	1.18, dd (15.1, 6.7); 2.17, dd (15.1, 12.9)	39.7
2	1.88, m	35.3	1.88, m	35.2
3	1.51, m	36.5	1.51, m	36.5
4	1.29, m; 1.53, m	26.4	1.29, m; 1.53, m	26.4
5	1.28, m; 1.36, m	39.7	1.28, m; 1.36, m	39.7
6	0.90, m; 2.20, m	38.8	0.90, m; 2.19, brd (13.9)	38.8
7	-	33.6	-	33.5
8	1.43, m; 2.84, dd (13.7, 8.3)	36.4	1.43, m; 2.83, dd (13.5, 8.4)	36.4
9	5.38, m	118.4	5.37, brt (8.4)	118.4
10	-	145.1	-	145.0
11	-	42.0	-	42.0
12	2.07, td (13.6, 5.1); 0.90, m	34.5	2.06, td (13.9, 5.1); 0.88, m	34.5
13	1.58, m; 1.63, m	36.7	1.58, m; 1.63, td (12.9, 3.9)	36.7
14	2.42, d (11.4)	53.2	2.42, d (11.2)	53.1
15	-	44.8	-	44.8
16	1.34, m; 1.51, m	39.7	1.32, m; 1.49, m	39.7
17	1.48, m; 2.02, m	29.3	1.49, m; 2.01, m	29.2
18	2.72, m	45.7	2.72, td (10.7, 7.6)	45.7
19	-	148.4	-	148.3
20	0.90, d (6.9)	19.7	0.88, d (6.7)	19.7
21	0.88, s	30.9	0.88, s	30.9
22	1.20, s	30.2	1.20, s	30.2
23	0.91, s	19.4	0.91, s	19.4
24	4.85, brs; 4.88, brs	110.2	4.85, brs; 4.88, brs	110.2

25	1.68, s	19.9	1.67, s	19.9

Table S3. 1D and 2D NMR Data of **2**.

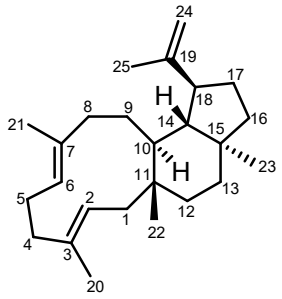

astellifatriene (**2**)

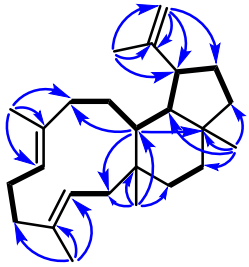

^{1}H-^{1}H COSY
Key HMBC

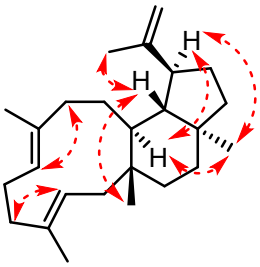

Key NOESY

Pos.	δ_H[a] mult (*J* in Hz)	δ_C[b]	COSY (^{1}H –^{1}H)	HMBC	NOESY
1a	1.74, m	39.1	2	12, 10, 2, 3	
1b	2.15, m		2	22, 12, 2, 3	
2	5.04, d (8.2)	125.0	1	3, 1, 4, 20	4a, 4b
3	-	132.5	-	-	
4a	1.94, m	39.7	5a, 5b	20, 5, 2, 3	2
4b	2.15, m		5a, 5b	20, 5, 2, 3	2
5a	2.00, m	26.3	6, 4a, 4b	6, 3, 7	
5b	2.26, qd (4.4, 12.8)		6, 4a, 4b	4, 6, 3, 7	
6	4.93, dd (3.7, 11.4)	124.5	5a, 5b	21, 5, 4, 8	8a, 8b
7	-	137.7	-	-	
8a	1.87, m	42.0	9b	21, 9, 10, 7, 6	6
8b	2.00, m		9a, 9b	6, 7	6
9a	1.21, m	24.3	8b, 10	10, 8, 14, 7	
9b	1.01, m		8a, 8b	10, 8, 14, 7	
10	1.64, m	39.8	9a, 14	22, 9, 1, 8, 15, 14	18, 23
11	-	39.1	-	-	
12a	2.00, m	34.7	13a, 13b	-	
12b	1.01, m		13a, 13b	22, 13, 15	
13a	1.51, m	36.3	12a, 12b	23, 12, 15, 14	
13b	1.43, m		12a, 12b	23, 12, 16, 15, 14	
14	1.58, t (11.3)	49.8	18, 10	23, 13, 10, 15, 18, 19	22, 25
15	-	43.9	-	-	
16a	1.42, m	40.4	17a	23, 15, 18, 14	
16b	1.21, m		17b	23, 17, 13, 15	
17a	2.00, m	30.7	16a	15, 18, 14, 19	
17b	1.46, m		16b	19	
18	2.69, td (5.2, 10.9)	47.5	17a, 17b, 14	25, 17, 10, 14, 24, 19	10, 23
19	-	148.6	-	-	
20	1.47, s	16.7	-	4, 3, 2	
21	1.45, s	16.9	-	8, 7, 6	
22	0.85, s	21.2	-	12, 1, 10, 11	14
23	0.87, s	18.0	-	13, 16, 15, 14	10, 18
24a	4.77, d (2.4)	110.5	-	25, 17, 18, 19	
24b	4.70, dd (1.3, 2.5)		-	25, 17, 18, 19	
25	1.70, s	19.1	-	18, 24, 19	14

[a]Recorded at 600 MHz in C_6D_6. [b]Recorded at 150 MHz in C_6D_6.

Table S4. Comparison of ^{1}H (600 MHz) and ^{13}C (150 MHz) NMR (in $CDCl_3$) data of astellifatriene (**2**) to those of **C1** (900 MHz, in $CDCl_3$) in the literature.[15]

Pos.	δ_H mult (*J* in Hz), astellifatriene (**2**)	δ_C, astellifatriene (**2**)	δ_H mult (*J* in Hz), **C1**	δ_C, **C1**
1	1.67, m; 2.10, dd (8.2, 16.5)	38.8	1.67, dd (16.6, 1.9); 2.11, dd (8.2, 16.6)	38.7
2	4.89, d (8.3)	124.8	4.89, d (8.2)	124.6
3	-	132.6	-	132.5
4	1.91, m; 2.18, m	39.4	1.93, o; 2.19, d (11.9)	39.2
5	2.02, m; 2.26, m	26.0	2.02, o; 2.26, dddd (12.9, 12.9, 12.9, 4.5)	25.8
6	4.79, dd (11.5, 3.9)	124.1	4.79, dd (12.9, 4.5)	124.0
7	-	138.0	-	137.8
8	1.70, m; 1.82, dd (12.9, 7.6)	41.7	1.70, dd (12.9, 12.9); 1.83, dd (12.9, 8.3)	41.5
9	0.96, m; 1.10, m	24.0	0.95, m; 1.10, m	23.8
10	1.53	39.5	1.53	39.4
11	-	38.9	-	38.8
12	1.00, m; 1.90, m	34.5	1.00, ddd (14.1, 4.3, 2.5); 1.91, o	34.3
13	1.43, m; 1.52 m	36.0	1.43, o; 1.51, o	35.9
14	1.55, m	49.6	1.55, 0	49.4
15	-	43.8	-	43.6
16	1.21, m; 1.43, m	40.2	1.21, ddd (10.9, 10.9, 10.9); 1.43, o	40.1
17	1.41, m; 2.00, m	30.5	1.40, o; 2.00, o	30.4
18	2.65, ddd (10.5, 10.5, 5.0)	47.3	2.66, ddd (10.8, 10.8, 5.3)	47.2
19	-	148.8	-	148.7
20	1.49, s	16.7	1.49, s	16.5
21	1.44, s	16.8	1.44, s	16.7
22	0.82, s	21.2	0.82, s	21.0
23	0.87, s	18.0	0.87, s	17.9
24	4.59, brs; 4.68, brs	110.1	4.60, dd (2.3, 1.3); 4.68, d (2.2)	109.9
25	1.72, s	19.1	1.72, s	18.9

Table S5. Measured specific rotation of compound **2** computed (Boltzmann-averaged and relative free energies computed at b3lyp/6-311g(d,p) level) specific rotation at different wavelengths.

Wavelength / Conformers	589 nm	546 nm	436 nm	405 nm
2-A (0.9%)	163.2	194.6	338.7	411.8
2-B (5.8%)	152.4	182.4	322.4	395.1
2-C (0.3%)	63.8	74.0	113.4	129.2
2-D (93.0%)	56.2	66.0	108.3	128.5
Boltzmann-averaged specific rotation	62.7	73.9	122.8	146.5
Mirrored Boltzmann-averaged specific rotation	-62.7	-73.9	-122.8	-146.5

Table S6. Relative production of the products from EvAS, and its variants. The calculation was based on GC-MS analysis. All data represent the mean of n = 3 biologically independent samples and error bars show standard deviation.

	Peak area of GC-MS analysis		Relative production (%)		
products	**1**	**2**	**1**	**2**	total
EvAS-WT	101065±5575	56781±4372	100%	56.2%	156.2%
I66A	5106±861	14102±2352	5.1%	13.9%	19%
S85A	0	25143±9388	0	24.9%	24.9%
S85N	0	187919±17532	0	185.9%	185.9%
S85L	0	0	0	0	0
S85Y	0	0	0	0	0
S85H	0	0	0	0	0
S85D	0	0	0	0	0
F89A	0	0	0	0	0
F187A	0	0	0	0	0
W188A	0	0	0	0	0
W310A	0	0	0	0	0
S303A	0	0	0	0	0
N307A	0	0	0	0	0

Table S7. Pocket volumes of EvAS and its variants predicted by POVME.[4]

TC-models	volume (Å^3)
EvAS-WT	302.4 ± 17.0
EvAS-S85A	244.2 ± 11.3
EvAS-S85N	230.1 ± 19.2
EvAS-S85D	88.8 ± 24.9
EvAS-S85Y	22.8 ± 8.2
EvAS-S85L	80.9 ± 25.1
EvAS-S85H	90.9 ± 29.6
EvAS-I66A	71.7 ± 21.3
EvAS-F89A	138.8 ± 36.1
EvAS-F187A	70.8 ± 17.3
EvAS-W188A	143.3 ± 22.2
EvAS-S303A	77.8 ± 16.2
EvAS-N307A	98.9 ± 28.8
EvAS-W310A	83.6 ± 15.0

Table S8. Primers for mutation in this study.

	Variants	Primers
Forward	I66A-F	AAGGTGGTCTGGCAGACCAGTGGAACGGT*GCA*TCTATC
	S85A-F	TCTGGGTGTTGTTAGCTACGCT*GCA*GAATTCGCGTTCG
	S85N-F	TCTGGGTGTTGTTAGCTACGCT*AAC*GAATTCGCGTTCG
	S85L-F	TCTGGGTGTTGTTAGCTACGCT*CTC*GAATTCGCGTTCG
	S85Y-F	TCTGGGTGTTGTTAGCTACGCT*TAC*GAATTCGCGTTCG
	S85H-F	TCTGGGTGTTGTTAGCTACGCT*CAC*GAATTCGCGTTCG
	S85D-F	TCTGGGTGTTGTTAGCTACGCT*GAT*GAATTCGCGTTCG
	F89A-F	TCTGGGTGTTGTTAGCTACGCTTCCGAATTCGCG*GCA*GT
	F187A-F	ACCGTATCTACGATGTTGGTATGCTG*GCA*TGGTACGG
	W188A-F	ACCGTATCTACGATGTTGGTATGCTGTTC*GCA*TACGGTCT
	W310A-F	GTACCTGGAAAGCCTGCTGTACTCCATGTCTGGTAACGTTGTT*GCA*GG
	S303A-F	GTACCTGGAAAGCCTGCTGTAC*GCA*ATGTCTGGTAACGTTGTTTGGGG
	N307A-F	GTACCTGGAAAGCCTGCTGTACTCCATGTCTGGT*GCA*GTTGTTTGGGG
Reverse	I66A-R	CTGGTCTGCCAGACCACCTTTGTAAACACCCAGCGGACCA
	S85A-R	CGTAGCTAACAACACCCAGACGGTCCGGCAAAGCTTCTG
	F187A-R	ACCAACATCGTAGATACGGTATTTCAAGAATTCTTTCTCGTTGTT
	S303A-R	ACAGCAGGCTTTCCAGGTACAGCATAGTGTCGTGAGAC

Table S9. Energy analysis for the conformers of (2*E*,6*E*,10*S*,11*R*,14*S*,15*S*,18*S*)-**2**.

conformers	Total Energy (Hartree)
2-A (0.9%)	-976.695215
2-B (5.8%)	-976.695881
2-C (0.3%)	-976.693488
2-D (93.0%)	-976.700851

Table S10. Cartesian coordinates for the conformers of (2*E*,6*E*,10*S*,11*R*,14*S*,15*S*,18*S*)-**2**.

	2-A				**2-B**				**2-C**				**2-D**		
C	-1.54406	2.202258	-0.27275	C	1.693633	2.142574	0.35005	C	1.955309	2.016489	0.452277	C	-2.08382	2.078977	-0.20094
C	-2.82202	2.01088	0.083626	C	2.944141	1.928577	-0.08252	C	3.072418	2.048139	-0.29045	C	-2.51983	1.501926	-1.33273
C	-2.59632	-1.24213	-0.23541	C	2.561663	-1.29339	0.152194	C	2.754602	-1.22588	-0.74099	C	-2.38598	-1.47007	-0.06748
C	-0.27407	-1.8533	0.76945	C	0.177846	-1.78026	-0.78001	C	0.14063	-1.7817	-0.77503	C	-0.06806	-1.57615	1.094241
C	0.228694	-0.40088	0.371161	C	-0.26742	-0.32577	-0.32454	C	-0.33727	-0.36799	-0.21623	C	0.348079	-0.24487	0.341869
C	-0.2309	0.690246	1.373764	C	0.196632	0.793658	-1.2946	C	0.236084	0.828332	-1.03304	C	-0.10464	1.054902	1.063481
C	-0.4511	2.113926	0.791134	C	0.541617	2.16662	-0.65135	C	0.605569	2.117404	-0.2475	C	-0.60173	2.181806	0.105674
C	-4.03824	1.821763	-0.7891	C	4.191408	1.65395	0.722093	C	4.463461	1.630509	0.091669	C	-3.9213	1.073226	-1.67606
C	-4.21992	0.324263	-1.2321	C	4.313694	0.14031	1.127472	C	4.765869	0.20354	-0.47696	C	-4.08654	-0.48088	-1.55447
C	-3.79184	-0.638	-0.14462	C	3.792658	-0.77066	0.037541	C	3.786751	-0.83741	0.028691	C	-3.63048	-0.98651	-0.20201
C	0.252938	-2.27655	2.159649	C	-0.41275	-2.15373	-2.15925	C	0.002819	-1.85233	-2.31257	C	0.477712	-1.60454	2.539961
C	-1.09566	2.468652	-1.68882	C	1.330742	2.3443	1.801321	C	1.922554	1.815754	1.947343	C	-2.98264	2.619109	0.887066
C	-4.70395	-0.73135	1.054045	C	4.657046	-0.89455	-1.19315	C	4.040475	-1.31065	1.441033	C	-4.5933	-0.78667	0.942412
C	-1.83861	-1.96059	0.851902	C	1.731499	-1.936	-0.9295	C	1.615679	-2.13283	-0.35594	C	-1.62236	-1.73965	1.205251
H	-0.25658	-0.16511	-0.58159	H	0.244287	-0.14023	0.625241	H	0.047895	-0.29646	0.810313	H	-0.17559	-0.26	-0.62054
C	0.191661	-2.8913	-0.29293	C	-0.28042	-2.82407	0.279784	C	-0.68386	-2.96379	-0.16243	C	0.463451	-2.82387	0.327465
C	2.126823	-1.43287	-1.0508	C	-2.16909	-1.33517	1.110264	C	-2.53515	-1.46605	0.654757	C	2.293108	-1.49602	-0.82809
C	1.759615	-0.45391	0.107239	C	-1.79405	-0.34621	-0.03556	C	-1.89072	-0.30635	-0.15643	C	1.871334	-0.27988	0.048598
H	2.227646	-0.88846	1.000581	H	-2.28014	-0.75689	-0.93059	H	-2.24455	-0.45528	-1.18702	H	2.376693	-0.43692	1.012237
C	3.651449	-1.22982	-1.13039	C	-3.69018	-1.10922	1.209691	C	-4.02073	-1.06534	0.617705	C	3.801707	-1.22856	-0.99579
C	3.842343	0.29783	-0.9986	C	-3.86445	0.419047	1.065676	C	-4.009	0.453505	0.891195	C	3.899909	0.296767	-1.22825
C	2.577832	0.830683	-0.21431	C	-2.59193	0.953156	0.301485	C	-2.61018	0.974908	0.371692	C	2.597561	0.935335	-0.61052
C	3.02584	1.720935	0.937617	C	-3.0115	1.839712	-0.8617	C	-2.83457	2.144356	-0.58069	C	2.945257	2.113951	0.285122
C	3.428159	3.118522	0.522281	C	-3.6187	1.182083	-2.08076	C	-3.02412	3.477753	0.106092	C	3.647946	1.834549	1.59544
C	3.158416	1.324408	2.208364	C	-2.93502	3.173423	-0.77533	C	-2.9731	2.036144	-1.90689	C	2.70996	3.371964	-0.10732
C	1.507971	-1.04542	-2.41396	C	-1.52745	-0.97884	2.470569	C	-2.07539	-1.52047	2.130216	C	1.636233	-1.50786	-2.22734
C	1.685854	-2.84766	-0.65171	C	-1.7625	-2.75296	0.68245	C	-2.20254	-2.77541	-0.06747	C	1.94984	-2.78216	-0.06344
H	-3.00616	1.841295	1.146065	H	3.070664	1.811399	-1.16045	H	2.944656	2.225656	-1.36182	H	-1.76138	1.178441	-2.04911
H	-2.06843	-1.12837	-1.18182	H	2.067981	-1.16388	1.114681	H	2.742637	-0.85453	-1.76557	H	-1.82485	-1.61424	-0.99029
H	0.483066	0.769584	2.200442	H	-0.56465	0.96491	-2.0663	H	-0.48563	1.096534	-1.81021	H	0.718701	1.445456	1.670921
H	-1.18321	0.382941	1.818898	H	1.092849	0.45806	-1.82757	H	1.14375	0.524759	-1.55421	H	-0.90992	0.829904	1.771468
H	0.488758	2.506533	0.391909	H	-0.34975	2.588675	-0.18093	H	-0.1796	2.373222	0.471925	H	-0.38626	3.15303	0.570669
H	-0.71182	2.767945	1.634304	H	0.792091	2.849175	-1.47491	H	0.63512	2.941655	-0.97187	H	-0.0243	2.151844	-0.82364
H	-4.92818	2.142017	-0.23321	H	5.068162	1.938238	0.127347	H	4.604725	1.629512	1.177647	H	-4.65775	1.565125	-1.03258
H	-4.00151	2.444097	-1.69078	H	4.234239	2.258153	1.635927	H	5.20961	2.323824	-0.32019	H	-4.17264	1.357867	-2.70719
H	-5.26741	0.170753	-1.52845	H	5.362742	-0.07325	1.377081	H	5.79766	-0.06557	-0.20874	H	-5.13838	-0.733	-1.74972
H	-3.60384	0.152993	-2.12237	H	3.725657	-0.01944	2.038612	H	4.724006	0.253881	-1.57227	H	-3.49172	-0.95485	-2.34523
H	-0.02408	-1.54983	2.931316	H	-0.15241	-1.40881	-2.91978	H	0.612149	-1.10432	-2.82755	H	0.149551	-0.73001	3.112623
H	-0.18263	-3.24192	2.446514	H	-0.00567	-3.11689	-2.49152	H	0.319836	-2.83823	-2.67386	H	0.108792	-2.49569	3.062884
H	1.340509	-2.39316	2.189357	H	-1.50221	-2.25233	-2.15074	H	-1.03357	-1.7054	-2.63688	H	1.57084	-1.63606	2.581886
H	-0.5287	3.408899	-1.74407	H	0.811673	3.303475	1.938995	H	1.358059	2.627727	2.4269	H	-2.8066	2.109647	1.844077
H	-0.42098	1.681454	-2.05252	H	0.638422	1.56802	2.155311	H	1.410064	0.882542	2.217804	H	-4.04655	2.531535	0.656508
H	-1.9306	2.54142	-2.39163	H	2.2022	2.338888	2.462233	H	2.917149	1.793437	2.40002	H	-2.76596	3.682616	1.060042
H	-5.68874	-1.11502	0.752467	H	5.632075	-1.32872	-0.93132	H	4.115793	-0.46935	2.142057	H	-5.48761	-1.40959	0.797567
H	-4.31759	-1.39485	1.831961	H	4.211193	-1.52886	-1.96358	H	3.272462	-1.98942	1.818435	H	-4.16245	-1.05339	1.911124
H	-4.88315	0.253263	1.508186	H	4.867275	0.085996	-1.64326	H	5.001568	-1.84203	1.492396	H	-4.94644	0.250854	1.003955
H	-2.07294	-3.03718	0.851896	H	1.926175	-3.01905	-0.98577	H	1.617513	-2.26522	0.731328	H	-1.80084	-2.767	1.56157
H	-2.17187	-1.59416	1.829609	H	2.037972	-1.53907	-1.90438	H	1.806081	-3.136	-0.77323	H	-1.99801	-1.08849	2.003582
H	-0.0639	-3.8956	0.07218	H	-0.05907	-3.82868	-0.1063	H	-0.4614	-3.86862	-0.7438	H	0.275571	-3.71172	0.946896
H	-0.40009	-2.75259	-1.20712	H	0.340981	-2.71121	1.177815	H	-0.30517	-3.16884	0.846283	H	-0.13601	-2.96867	-0.57969
H	4.091677	-1.63225	-2.05066	H	-4.12114	-1.49882	2.139824	H	-4.63467	-1.62045	1.33727	H	4.251846	-1.81043	-1.80908
H	4.13343	-1.7454	-0.28933	H	-4.19117	-1.62832	0.381562	H	-4.42981	-1.26699	-0.3813	H	4.326998	-1.50704	-0.07232
H	4.767217	0.540555	-0.46636	H	-4.78658	0.672206	0.532953	H	-4.83397	0.96136	0.382825	H	4.805556	0.715786	-0.77849
H	3.911437	0.771312	-1.98396	H	-3.93578	0.906474	2.043757	H	-4.12296	0.658448	1.961174	H	3.954157	0.534881	-2.29576
H	1.997739	1.457733	-0.90343	H	-2.01027	1.570889	0.994525	H	-2.05082	1.357705	1.235231	H	1.982744	1.319503	-1.43206
H	2.581081	3.659877	0.079113	H	-4.4203	0.483243	-1.80646	H	-2.12263	3.769169	0.661677	H	4.519187	1.180666	1.457817
H	3.800474	3.704178	1.368427	H	-4.04152	1.928054	-2.7605	H	-3.25734	4.274796	-0.60666	H	3.994438	2.76183	2.061734
H	4.214444	3.091494	-0.24456	H	-2.87778	0.600416	-2.64332	H	-3.8402	3.429181	0.840418	H	2.989511	1.327507	2.312094
H	3.545083	1.999184	2.96822	H	-3.29278	3.821369	-1.57199	H	-3.20626	2.903782	-2.51918	H	3.007629	4.225941	0.496712
H	2.89687	0.326982	2.54712	H	-2.51556	3.669142	0.097035	H	-2.86729	1.094801	-2.43763	H	2.212782	3.59592	-1.04791
H	1.788413	-0.03327	-2.72421	H	-1.78131	0.036507	2.793714	H	-2.32596	-0.60286	2.672333	H	1.864156	-0.6013	-2.7978
H	1.868036	-1.73456	-3.18809	H	-1.89483	-1.66776	3.241336	H	-2.57788	-2.35015	2.643349	H	2.016668	-2.36027	-2.80388
H	0.415644	-1.09507	-2.41973	H	-0.43637	-1.05423	2.463123	H	-0.99856	-1.67302	2.239812	H	0.547323	-1.60102	-2.19017
H	1.889299	-3.56333	-1.46076	H	-1.95782	-3.47462	1.488156	H	-2.64256	-3.63838	0.452286	H	2.195365	-3.67089	-0.66176
H	2.286104	-3.17795	0.207507	H	-2.39231	-3.06173	-0.16349	H	-2.65354	-2.75476	-1.06973	H	2.576205	-2.83679	0.837948

Table S11. The Gibbs free energy profiles for reprotonation sequences mediated by hydroxyl oxygen and carbonyl oxygen of serine, progressing from state **2** to **IM3**.

	Thermal correction to Gibbs Free Energy (B3LYP/6-31G(d))	Total energy/Hartree (mPW1PW91/6-311+G(d,p))	Imaginary Freq
2_S-O_H	0.654343	-1300.86511	none
TS1	0.649553	-1300.850884	-785.23
IM3_S-O	0.657684	-1300.869387	none
2_S=O_H	0.655674	-1300.85144	none
TS2	0.650079	-1300.842604	-983.87
IM3_S=O	0.655953	-1300.85996	none

Table S12. Cartesian coordinates of the intermediates and transition states for reprotonation sequences mediated by hydroxyl oxygen and carbonyl oxygen of serine, progressing from state **2** to **IM3**.

2_S-O_H				**TS1**				**IM3_S-O**			
C	-5.63892	-2.10518	-0.09275	C	-6.01483	-1.88204	-0.62277	C	-3.46528	-3.25746	-1.25337
C	-4.24144	-1.50916	-0.32674	C	-4.70773	-1.20056	-1.03881	C	-3.40328	-2.00633	-2.1452
O	-4.07073	-0.48175	0.65852	O	-3.99437	-0.7798	0.154804	O	-2.45389	-1.06406	-1.65473
H	-4.15821	-1.0987	-1.34142	H	-4.90665	-0.32966	-1.67386	H	-4.40383	-1.55176	-2.21194
H	-3.48661	-2.29151	-0.20409	H	-4.05783	-1.89317	-1.57632	H	-3.0987	-2.28757	-3.15731
C	1.308043	3.124288	-0.55073	C	0.902534	3.023442	-0.55865	C	-0.25216	2.612609	-1.43872
C	0.448726	2.719949	-1.50272	C	0.094036	2.51554	-1.51312	C	-1.40315	1.842245	-1.00186
C	-1.25271	0.552698	0.324002	C	-1.12145	0.33024	0.218564	C	-1.41413	1.588493	0.648069
C	0.711555	-0.64522	1.551508	C	0.909353	-0.61267	1.538519	C	1.060614	1.102686	1.530099
C	1.681602	0.006417	0.480957	C	1.846339	0.070957	0.46299	C	1.449468	0.527005	0.11476
C	2.355593	1.326611	0.92647	C	2.372195	1.476669	0.844601	C	1.965228	1.574845	-0.89553
C	2.566691	2.330026	-0.24701	C	2.303505	2.4803	-0.34268	C	0.912626	1.945031	-2.03192
C	-0.94113	3.224995	-1.78739	C	-1.34284	2.854316	-1.79693	C	-2.80397	2.467511	-1.29285
C	-2.03239	2.169322	-1.3959	C	-2.30863	1.658434	-1.50987	C	-3.68328	1.994096	-0.12607
C	-1.86827	1.725796	0.043245	C	-2.17465	1.183493	-0.06291	C	-2.78755	2.162285	1.108564
C	1.321844	-0.61554	2.971133	C	1.466338	-0.47132	2.972816	C	2.185575	1.975158	2.138601
C	1.113331	4.33876	0.326895	C	0.525432	4.152902	0.370709	C	-0.18182	4.08448	-1.29404
C	-2.25016	2.738787	1.097545	C	-2.75206	2.097885	1.009497	C	-2.78702	3.604249	1.638812
C	-0.64828	0.132967	1.647324	C	-0.49302	0.077489	1.550484	C	-0.19815	2.025181	1.478653
C	0.465255	-2.16326	1.217514	C	0.787569	-2.15647	1.263799	C	0.855876	-0.09937	2.535349
C	0.558219	-2.57827	-0.2607	C	0.967512	-2.62596	-0.19087	C	0.518907	-1.47824	1.937409
C	1.87297	-2.10523	-0.94492	C	2.253539	-2.06598	-0.86572	C	1.482281	-1.91598	0.796237
C	2.629365	-1.11463	-0.00988	C	2.90065	-0.97824	0.043515	C	2.355847	-0.70372	0.356052
C	2.972815	-3.1687	-1.15032	C	3.450372	-3.03018	-1.01199	C	2.606333	-2.91924	1.136213
C	4.278159	-2.33854	-1.30668	C	4.67531	-2.08669	-1.18322	C	3.65307	-2.70783	0.001023
C	3.98315	-0.89634	-0.73692	C	4.238903	-0.65847	-0.67128	C	3.330574	-1.31821	-0.67627
C	1.516114	-1.51042	-2.32646	C	1.877741	-1.55804	-2.2774	C	0.6313	-2.52922	-0.34061
C	5.14091	-0.35462	0.084305	C	5.325455	0.021004	0.145018	C	4.580672	-0.52684	-1.02236
C	5.451667	-1.00645	1.413115	C	5.674381	-0.55004	1.501138	C	5.423373	0.028503	0.103047
C	5.899673	0.644142	-0.38374	C	5.989092	1.073627	-0.34929	C	4.946224	-0.36118	-2.30164
H	1.14268	4.074265	1.392417	H	0.680028	3.875811	1.421519	H	0.847718	4.430244	-1.15563
H	1.936813	5.047425	0.166194	H	1.179297	5.015178	0.184971	H	-0.51442	4.504853	-2.26002
H	0.180852	4.87583	0.136913	H	-0.50562	4.495213	0.258734	H	-0.83724	4.488422	-0.52221
H	-2.25735	2.32057	2.106769	H	-2.79991	1.610999	1.98784	H	-2.10922	3.736372	2.487259
H	-1.55689	3.588257	1.095203	H	-2.14303	3.001789	1.119976	H	-2.51282	4.34175	0.875373
H	-3.24626	3.151943	0.892931	H	-3.76469	2.416033	0.740657	H	-3.79325	3.864525	1.98373
H	2.2956	-1.11703	2.997223	H	2.484257	-0.86924	3.039729	H	3.13868	1.438974	2.187819
H	1.460752	0.403054	3.346076	H	1.491412	0.566895	3.31805	H	2.352984	2.908614	1.589839
H	0.667856	-1.14083	3.678601	H	0.84876	-1.0388	3.679779	H	1.921179	2.255428	3.164912
H	0.970196	-2.26059	-2.91225	H	1.407442	-2.3738	-2.83966	H	0.039986	-3.35375	0.077278
H	0.871788	-0.62673	-2.24745	H	1.160166	-0.72809	-2.2509	H	-0.08195	-1.82497	-0.78403
H	2.396015	-1.2258	-2.9107	H	2.742358	-1.22454	-2.8581	H	1.235118	-2.94959	-1.15041
H	3.033483	-3.81846	-0.26776	H	3.555353	-3.63707	-0.10366	H	3.04427	-2.68115	2.113686
H	2.781812	-3.81721	-2.01337	H	3.336082	-3.72583	-1.85104	H	2.250442	-3.9541	1.187096
H	5.110275	-2.8098	-0.77549	H	5.538893	-2.45807	-0.62408	H	4.672134	-2.72235	0.398243
H	4.588274	-2.26629	-2.35374	H	4.994272	-2.02378	-2.22803	H	3.606517	-3.50374	-0.74807
H	3.844327	-0.21611	-1.58366	H	4.047854	-0.0222	-1.54244	H	2.799233	-1.5038	-1.61684
H	2.899157	-1.70347	0.878032	H	3.201988	-1.50452	0.960062	H	2.986722	-0.46829	1.222575
H	1.052411	0.282282	-0.36988	H	1.219652	0.234437	-0.41978	H	0.530071	0.116733	-0.31693
H	1.744651	1.823857	1.689875	H	1.798014	1.896265	1.678557	H	2.299467	2.499255	-0.4177
H	3.321133	1.124303	1.399531	H	3.40662	1.419412	1.192638	H	2.820652	1.191987	-1.45966
H	2.897651	1.786317	-1.13767	H	2.670165	1.993012	-1.25274	H	0.62846	1.019258	-2.53881
H	3.381634	3.014371	0.019975	H	2.986536	3.313695	-0.13579	H	1.427944	2.615384	-2.72886
H	0.741938	1.857076	-2.10368	H	0.516624	1.75192	-2.16883	H	-1.36786	0.849319	-1.45135
H	-1.03332	-0.09267	-0.5268	H	-0.76147	-0.26501	-0.61862	H	-1.4941	0.499305	0.695715
H	-3.23687	0.042169	0.477074	H	-2.97843	0.07422	0.00196	H	-3.13225	1.509276	1.921915
H	-1.93425	1.305677	-2.06634	H	-2.0656	0.838072	-2.19746	H	-3.93836	0.938094	-0.26486
H	-3.02116	2.614564	-1.57292	H	-3.3376	1.971141	-1.7225	H	-4.61814	2.560152	-0.06019
H	-1.14512	4.162847	-1.26259	H	-1.67466	3.727982	-1.22944	H	-2.76217	3.560319	-1.32198
H	-1.06582	3.436773	-2.8578	H	-1.4666	3.110218	-2.85765	H	-3.15967	2.123206	-2.26804
H	1.197388	-2.7576	1.777124	H	1.542766	-2.66328	1.875283	H	1.77774	-0.20377	3.119479
H	-0.51018	-2.46393	1.62438	H	-0.17567	-2.51654	1.649586	H	0.085206	0.173122	3.26692
H	0.459388	-3.66993	-0.3321	H	0.969233	-3.72343	-0.20845	H	0.523408	-2.21826	2.748078
H	-0.3011	-2.17171	-0.81233	H	0.090032	-2.33319	-0.78454	H	-0.51147	-1.47477	1.558551
H	-0.49131	1.030293	2.255284	H	-0.43163	1.037811	2.078061	H	0.10437	3.040641	1.193484
H	-1.3438	-0.49564	2.224122	H	-1.18151	-0.53449	2.156365	H	-0.54799	2.132671	2.5127

H	6.761134	1.015779	0.165415	H	6.801547	1.547101	0.195952	H	5.859591	0.161057	-2.57473
H	5.693814	1.121726	-1.3388	H	5.753791	1.493407	-1.32469	H	4.35707	-0.76493	-3.12231
H	6.394715	-0.63357	1.82294	H	6.570157	-0.07407	1.909839	H	6.365665	0.435981	-0.27366
H	4.667512	-0.81024	2.156266	H	4.862494	-0.40271	2.226092	H	4.905672	0.834133	0.640264
H	5.532832	-2.09754	1.325748	H	5.860544	-1.63059	1.455997	H	5.664774	-0.73867	0.849111
H	-5.43277	0.162513	0.587195	H	-4.72488	-0.35429	0.71774	H	-2.62266	-1.06044	-0.68623
C	-6.70656	-1.04103	-0.10141	C	-6.85493	-0.95592	0.253512	C	-3.81715	-2.90124	0.187486
O	-6.44462	0.141068	0.333764	O	-6.30641	-0.11352	0.985668	O	-3.41226	-1.85453	0.717101
H	-5.86093	-2.88335	-0.82878	H	-6.56206	-2.19942	-1.51707	H	-4.17528	-3.98215	-1.66824
N	-7.92819	-1.28741	-0.52081	N	-8.18854	-1.10229	0.216345	N	-4.57347	-3.78795	0.868214
H	-8.63762	-0.56123	-0.47364	H	-8.7591	-0.53632	0.832596	H	-4.79198	-3.60011	1.838064
H	-8.19684	-2.19672	-0.87543	H	-8.64664	-1.7838	-0.3713	H	-4.917	-4.64131	0.453268
H	-5.66452	-2.57089	0.902409	H	-5.78756	-2.78458	-0.04114	H	-2.47742	-3.73646	-1.24159

2_S=O_H				**TS2**				**IM3_S=O**			
C	-5.46693	-0.82453	0.559363	C	-5.84544	-0.55635	0.051904	C	-5.55334	-1.60799	0.814209
C	-4.67255	-2.05298	0.260227	C	-4.9616	-1.63887	0.611528	C	-4.28976	-2.42747	0.578434
O	-3.42758	-2.00786	-0.07421	O	-3.70496	-1.5254	0.676718	O	-3.26078	-1.90459	0.145941
C	-5.83399	-0.03968	-0.74591	C	-5.78337	-0.5071	-1.50263	C	-6.0276	-0.90887	-0.47503
O	-6.20053	1.2795	-0.43714	O	-6.21208	0.744135	-1.98648	O	-6.80957	0.245352	-0.21116
H	-6.37013	-1.08066	1.121711	H	-6.87938	-0.68104	0.390954	H	-6.35876	-2.20865	1.2542
H	-6.61442	-0.57935	-1.29812	H	-6.35702	-1.3411	-1.92973	H	-6.56114	-1.62015	-1.12261
H	-4.95167	0.024722	-1.38812	H	-4.74559	-0.6199	-1.82744	H	-5.15425	-0.55389	-1.02585
C	0.605737	3.096782	-0.24026	C	0.457631	2.998543	-0.18748	C	0.427261	3.048089	0.225445
C	-0.11586	2.644671	-1.28136	C	-0.38768	2.493415	-1.11014	C	-0.37368	2.540359	-0.87132
C	-1.43171	-0.00291	0.178775	C	-1.24632	0.040461	0.492996	C	-1.12054	1.086788	-0.47204
C	0.685771	-0.92046	1.39701	C	0.975484	-0.80744	1.539519	C	0.560383	-0.47994	0.877448
C	1.557447	0.020871	0.468005	C	1.740761	0.065046	0.464592	C	1.777199	0.260661	0.204301
C	1.94384	1.382993	1.093897	C	2.166204	1.475329	0.942072	C	2.274707	1.513719	0.957412
C	1.988483	2.539891	0.051561	C	1.913182	2.570177	-0.13463	C	1.886491	2.879904	0.237632
C	-1.56359	2.905901	-1.60195	C	-1.86959	2.710707	-1.23919	C	-1.55852	3.436421	-1.35249
C	-2.44856	1.623478	-1.4101	C	-2.69281	1.403586	-0.9907	C	-2.6558	2.446395	-1.7756
C	-2.26694	1.049929	-0.02105	C	-2.37955	0.823499	0.386762	C	-2.63357	1.377685	-0.67592
C	1.218808	-0.94716	2.847541	C	1.647929	-0.74263	2.929136	C	0.811897	-0.77872	2.374782
C	0.134972	4.138465	0.747915	C	0.072347	4.013514	0.863201	C	-0.1802	3.721277	1.396119
C	-2.88803	1.838512	1.107296	C	-2.90279	1.592062	1.592455	C	-3.43663	1.796955	0.564912
C	-0.79719	-0.41866	1.493212	C	-0.47825	-0.26844	1.738164	C	-0.74875	0.368983	0.831659
C	0.741957	-2.40708	0.883558	C	0.973662	-2.32368	1.121214	C	0.361017	-1.88579	0.184313
C	0.983848	-2.62089	-0.62065	C	1.064928	-2.63709	-0.38305	C	0.902625	-2.0478	-1.24839
C	2.212775	-1.83496	-1.16079	C	2.225748	-1.88832	-1.1006	C	2.3769	-1.58128	-1.42421
C	2.723414	-0.83919	-0.07662	C	2.846699	-0.82744	-0.14293	C	2.835106	-0.80908	-0.15113
C	3.505138	-2.64258	-1.40731	C	3.490286	-2.7071	-1.43835	C	3.48144	-2.65988	-1.4737
C	4.631172	-1.57043	-1.3882	C	4.60009	-1.63127	-1.61363	C	4.780102	-1.88711	-1.09319
C	4.039454	-0.28667	-0.68566	C	4.078794	-0.30815	-0.92824	C	4.333903	-0.53273	-0.4156
C	1.810051	-1.15763	-2.49088	C	1.677179	-1.29564	-2.41949	C	2.467273	-0.75429	-2.7285
C	5.033642	0.361111	0.263109	C	5.165586	0.402026	-0.13885	C	5.197375	-0.15427	0.776074
C	5.408944	-0.37498	1.529818	C	5.690245	-0.25276	1.119358	C	5.116964	-0.99893	2.027133
C	5.602244	1.533966	-0.04274	C	5.677608	1.559258	-0.57632	C	6.040093	0.88583	0.701096
H	0.189011	3.767098	1.780064	H	0.35799	3.678036	1.868651	H	0.399571	3.545337	2.308106
H	0.796222	5.014166	0.705112	H	0.620596	4.9488	0.688742	H	-0.11128	4.806102	1.19925
H	-0.88305	4.492254	0.566899	H	-0.99226	4.257539	0.875999	H	-1.23223	3.483059	1.551372
H	-2.87516	1.30264	2.060502	H	-2.9345	0.974071	2.49482	H	-3.30547	1.092553	1.390907
H	-2.34448	2.779046	1.258493	H	-2.26427	2.456291	1.807727	H	-3.1771	2.798191	0.929655
H	-3.92268	2.111917	0.867227	H	-3.91087	1.975978	1.40489	H	-4.50387	1.811787	0.318796
H	2.269299	-1.25576	2.878886	H	2.69959	-1.04208	2.871333	H	1.739805	-1.33917	2.529742
H	1.142543	0.026566	3.341156	H	1.61039	0.257448	3.371959	H	0.856533	0.123778	2.994861
H	0.651926	-1.66829	3.449934	H	1.152466	-1.43046	3.625455	H	-0.00587	-1.39285	2.769189
H	1.442391	-1.92108	-3.18751	H	1.237728	-2.1011	-3.02017	H	2.082312	-1.35687	-3.55928
H	1.006114	-0.42321	-2.36054	H	0.888934	-0.55074	-2.25256	H	1.860938	0.160774	-2.69489
H	2.644227	-0.6492	-2.98295	H	2.450076	-0.8231	-3.03213	H	3.489584	-0.46471	-2.98829
H	3.651804	-3.36925	-0.59783	H	3.733815	-3.37989	-0.60615	H	3.271798	-3.447	-0.7387
H	3.480439	-3.20857	-2.3457	H	3.366935	-3.33179	-2.33029	H	3.557156	-3.14599	-2.45246
H	5.515322	-1.93737	-0.85882	H	5.542029	-1.96129	-1.16625	H	5.40365	-2.47695	-0.41514
H	4.965672	-1.3176	-2.39902	H	4.815496	-1.44097	-2.66942	H	5.399059	-1.67578	-1.97011
H	3.807703	0.451379	-1.46064	H	3.750651	0.381725	-1.7134	H	4.434018	0.273769	-1.15155
H	3.061861	-1.46836	0.75861	H	3.278624	-1.40147	0.688895	H	2.82713	-1.54874	0.659441
H	0.926007	0.270788	-0.38925	H	1.022511	0.244899	-0.34197	H	1.415277	0.619296	-0.76458
H	1.225252	1.660172	1.875229	H	1.623014	1.760452	1.850584	H	1.924029	1.556195	1.991616
H	2.915992	1.315358	1.590814	H	3.225585	1.487199	1.210705	H	3.367464	1.548182	0.997424
H	2.457938	2.182715	-0.87064	H	2.239965	2.201199	-1.11292	H	2.296519	2.851109	-0.77549
H	2.634007	3.337087	0.440551	H	2.539489	3.440646	0.09748	H	2.360155	3.684841	0.810457
H	0.369567	1.934962	-1.95355	H	0.03759	1.826046	-1.86212	H	0.280341	2.312162	-1.71486
H	-1.02434	-0.47004	-0.71803	H	-0.92247	-0.4491	-0.42335	H	-0.79864	0.464784	-1.31221
H	-2.97083	-1.08412	-0.00882	H	-3.03666	-0.42154	0.455842	H	-3.05651	0.428041	-1.02508
H	-2.15377	0.882212	-2.16342	H	-2.43352	0.674126	-1.76877	H	-2.40426	2.00476	-2.7478
H	-3.49384	1.901213	-1.59889	H	-3.75868	1.632104	-1.10011	H	-3.62827	2.937823	-1.88003
H	-1.97363	3.717335	-0.99395	H	-2.22608	3.493757	-0.56401	H	-1.92028	4.078855	-0.54477
H	-1.67934	3.216126	-2.64876	H	-2.11527	3.045206	-2.25577	H	-1.22316	4.091933	-2.16192
H	1.542245	-2.92226	1.427847	H	1.824205	-2.80599	1.616409	H	0.852806	-2.6371	0.81409
H	-0.18038	-2.92391	1.182945	H	0.085825	-2.81279	1.544266	H	-0.7042	-2.14226	0.196333
H	1.100874	-3.69593	-0.81182	H	1.169643	-3.72234	-0.51014	H	0.793554	-3.09808	-1.54765
H	0.088475	-2.32409	-1.18353	H	0.113552	-2.38378	-0.87109	H	0.263877	-1.48644	-1.94343
H	-0.83002	0.437516	2.175685	H	-0.45617	0.640616	2.352551	H	-0.75639	1.079182	1.668625
H	-1.37349	-1.21428	1.990189	H	-1.04767	-1.00126	2.33289	H	-1.57886	-0.31669	1.035414
H	6.351045	1.992738	0.598033	H	6.487323	2.062289	-0.05391	H	6.700469	1.150098	1.523027

H	5.348773	2.074549	-0.95168	H	5.314998	2.040771	-1.48162	H	6.119113	1.495276	-0.19668
H	6.243326	0.116876	2.037911	H	6.568577	0.275477	1.500848	H	5.889613	-0.71325	2.746321
H	4.571114	-0.4205	2.238244	H	4.936984	-0.26095	1.918696	H	4.144589	-0.89547	2.526617
H	5.704359	-1.41272	1.328812	H	5.976369	-1.29849	0.94926	H	5.24243	-2.06637	1.807277
H	-7.14003	1.316051	-0.19866	H	-7.18144	0.777323	-1.9852	H	-7.66779	-0.03517	0.142867
N	-5.23027	-3.24607	0.260662	N	-5.51954	-2.78459	1.001099	N	-4.36173	-3.75066	0.866784
H	-6.20144	-3.37756	0.51344	H	-6.51934	-2.93072	0.976109	H	-5.20299	-4.18836	1.210613
H	-4.68056	-4.06679	0.02262	H	-4.93279	-3.53542	1.346694	H	-3.5463	-4.32875	0.713829
H	-4.85758	-0.16005	1.178672	H	-5.4858	0.405487	0.427053	H	-5.29343	-0.82432	1.534515

References

1. Y. Matsuda, T. Mitsuhashi, S. Lee, M. Hoshino, T. Mori, M. Okada, H. Zhang, F. Hayashi, M. Fujita and I. Abe, *Angew. Chem. Int. Ed.*, 2016, **55**, 5785-5788.
2. P. Cramer, *Nat Struct Mol Biol*, 2021, **28**, 704-705.
3. M. Ma, M. Xu, H. Xu, Z. Lei, B. Xing, J. S. Dickschat and D. Yang, *Angew. Chem. Int. Ed.*, 2024, **63**, e202405140.
4. J. R. Wagner, J. Sorensen, N. Hensley, C. Wong, C. Zhu, T. Perison and R. E. Amaro, *J Chem Theory Comput*, 2017, **13**, 4584-4592.
5. P. Wang, X. Gao and Y. Tang, *Curr Opin Chem Biol*, 2012, **16**, 362-369.
6. G. W. T. M. J. Frisch, H. B. Schlegel, G. E. Scuseria, M. A. Robb, J. R. Cheeseman, G. Scalmani, V. Barone, G. A. Petersson, H. Nakatsuji, X. Li, M. Caricato, A. V. Marenich, J. Bloino, B. G. Janesko, R. Gomperts, B. Mennucci, H. P. Hratchian, J. V. Ortiz, A. F. Izmaylov, J. L. Sonnenberg, D. Williams-Young, F. Ding, F. Lipparini, F. Egidi, J. Goings, B. Peng, A. Petrone, T. Henderson, D. Ranasinghe, V. G. Zakrzewski, J. Gao, N. Rega, G. Zheng, W. Liang, M. Hada, M. Ehara, K. Toyota, R. Fukuda, J. Hasegawa, M. Ishida, T. Nakajima, Y. Honda, O. Kitao, H. Nakai, T. Vreven, K. Throssell, J. A. Montgomery, Jr., J. E. Peralta, F. Ogliaro, M. J. Bearpark, J. J. Heyd, E. N. Brothers, K. N. Kudin, V. N. Staroverov, T. A. Keith, R. Kobayashi, J. Normand, K. Raghavachari, A. P. Rendell, J. C. Burant, S. S. Iyengar, J. Tomasi, M. Cossi, J. M. Millam, M. Klene, C. Adamo, R. Cammi, J. W. Ochterski, R. L. Martin, K. Morokuma, O. Farkas, J. B. Foresman, D. J. Fox, Gaussian 09, Revision A.02, Gaussian, Inc., Wallingford CT., 2016.
7. L.-L. Sun, W.-S. Li, J. Li, H.-Y. Zhang, L.-G. Yao, H. Luo, Y.-W. Guo and X.-W. Li, *J. Org. Chem.*, 2021, **86**, 3367-3376.
8. Y. Zhang and J. Skolnick, *Proteins*, 2004, **57**, 702-710.
9. G. M. Morris, R. Huey, W. Lindstrom, M. F. Sanner, R. K. Belew, D. S. Goodsell and A. J. Olson, *J. Comput. Chem.*, 2009, **30**, 2785-2791.
10. Y. Duan, C. Wu, S. Chowdhury, M.C. Lee, G. Xiong, W. Zhang, R. Yang, P. Cieplak, R. Luo, T. Lee, J. Caldwell, J. Wang, P. A. Kollman, *J. Comput. Chem.*, 2003, **24**, 1999–2012.
11. W. L. Jorgensen, J. Chandrasekhar, J. D. Madura, R. W. Impey and M. L. Klein, *J. Chem. Phys.*, 1983, **79**, 926-935.
12. J. Wang, R. M. Wolf, J. W. Caldwell, P. A. Kollman and D. A. Case, *J. Comput. Chem.*, 2004, **25**, 1157-1174.
13. C. I. Bayly, P. Cieplak, W. Cornell, and P. A. Kollman, *J. Phys. Chem.*, 1993, **97**, 10269-10280.
14. D. A. Case, K. Belfon, I. Y. Ben-Shalom, S. R. Brozell, D. S. Cerutti, T. E. I. Cheatham, V. W. D. Cruzeiro, T. A. Darden, R. E. Duke, G. Giambasu, M. K. Gilson, H. Gohlke, A. W. Goetz, R. Harris, S. Izadi, S. A. Izmailov, K. Kasavajhala, A. Kovalenko, R. Krasny, T. Kurtzman, T. S. Lee, S. LeGrand, P. Li, C. Lin, J. Liu, T. Luchko, R. Luo, V. Man, K. M. Merz, Y. Miao, O. Mikhailovskii, G. Monard, H. Nguyen, A. Onufriev, F. Pan, S. Pantano, R. Qi, D. R. Roe, A. Roitberg, C. Sagui, S. Schott-Verdugo, J. Shen, C. Simmerling, N. R. Skrynnikov, J. Smith, J. Swails, R. C. Walker, J. Wang, L. Wilson, R. M. Wolf, X. Wu, Y. Xiong, Y. Xue, D. M. York, P. A. Kollman, AMBER 2020, University of California, San Francisco. 2020.
15. Q. Chen, J. Li, Z. Liu, T. Mitsuhashi, Y. Zhang, H. Liu, Y. Ma, J. He, T. Shinada, T. Sato, Y. Wang, H. Liu, I. Abe, P. Zhang and G. Wang, *Plant Commun.*, 2020, **1**, 100051.
16. A. Minami, T. Ozaki, C. Liu and H. Oikawa, *Nat. Prod. Rep.*, 2018, **35**, 1330-1346.
17. H. Sato, K. Saito and M. Yamazaki, *Front Plant Sci.*, 2019, **10**, 802.
18. K. A. Taizoumbe, B. Goldfuss and J. S. Dickschat, *Angew. Chem. Int. Ed.*, 2024, **63**, e202318375.

19. Y. Luo, X. Ma, Y. Qiu, Y. Lu, S. Shen, Y. Li, H. Gao, K. Chen, J. Zhou, T. Hu, L. Tu, H. Zhao, D. Li, F. Leng, W. Gao, T. Jiang, C. Liu, L. Huang, R. Wu and Y. Tong, *Angew. Chem. Int. Ed.*, 2023, **62**, e202313429.
20. J. Y. Liu, F. L. Lin, K. A. Taizoumbe, J. M. Lv, Y. H. Wang, G. Q. Wang, G. D. Chen, X. S. Yao, D. Hu, H. Gao and J. S. Dickschat, *Angew. Chem. Int. Ed.*, 2024, e202407895.
21. R. Chiba, A. Minami, K. Gomi and H. Oikawa, *Org. Lett.*, 2013, **15**, 594-597.
22. H. Chai, R. Yin, Y. Liu, H. Meng, X. Zhou, G. Zhou, X. Bi, X. Yang, T. Zhu, W. Zhu, Z. Deng and K. Hong, *Sci. Rep.*, 2016, **6**, 27181.
23. R. Chen, Q. Jia, X. Mu, B. Hu, X. Sun, Z. Deng, F. Chen, G. Bian and T. Liu, *Proc. Natl. Acad. Sci. U. S. A.*, 2021, **118**, e2023247118.
24. B. Qin, Y. Matsuda, T. Mori, M. Okada, Z. Quan, T. Mitsuhashi, T. Wakimoto and I. Abe, *Angew. Chem. Int. Ed.*, 2016, **55**, 1658-1661.
25. K. Narita, H. Sato, A. Minami, K. Kudo, L. Gao, C. Liu, T. Ozaki, M. Kodama, X. Lei, T. Taniguchi, K. Monde, M. Yamazaki, M. Uchiyama and H. Oikawa, *Org. Lett.*, 2017, **19**, 6696-6699.
26. L. Gao, K. Narita, T. Ozaki, N. Kumakura, P. Gan, A. Minami, C. Liu, X. Lei, K. Shirasu and H. Oikawa, *Tetrahedron Lett.*, 2018, **59**, 1136-1139.
27. G. Bian, Y. Han, A. Hou, Y. Yuan, X. Liu, Z. Deng and T. Liu, *Metab. Eng.*, 2017, **42**, 1-8.
28. Y. Ye, A. Minami, A. Mandi, C. Liu, T. Taniguchi, T. Kuzuyama, K. Monde, K. Gomi and H. Oikawa, *J. Am. Chem. Soc.*, 2015, **137**, 11846-11853.
29. T. Mitsuhashi, J. Rinkel, M. Okada, I. Abe and J. S. Dickschat, *Chemistry*, 2017, **23**, 10053-10057.
30. J. H. Huang, J. M. Lv, Q. Z. Wang, J. Zhou, Y. J. Lu, Q. L. Wang, D. N. Chen, X. S. Yao, H. Gao, and D. Hu, *Org. Biomol. Chem.*, 2019, **17**, 248-251.
31. L. Jiang, H. Yang, X. Zhang, X. Li, K. Lv, W. Zhang, G. Zhu, C. Liu, Y. Wang, T. Hsiang, L. Zhang and X. Liu, *Appl. Microbiol. Biotechnol.*, 2022, **106**, 6047-6057.
32. Y. Matsuda, T. Mitsuhashi, Z. Quan and I. Abe, *Org. Lett.*, 2015, **17**, 4644-4647.
33. M. Okada, Y. Matsuda, T. Mitsuhashi, S. Hoshino, T. Mori, K. Nakagawa, Z. Quan, B. Qin, H. Zhang, F. Hayashi, H. Kawaide and I. Abe, *J. Am. Chem. Soc*., 2016, **138**, 10011-10018.
34. Z. Quan and J. S. Dickschat, *Org. Lett.*, 2020, **22**, 7552-7555.
35. J. Guo, Y. S. Cai, F. Cheng, C. Yang, W. Zhang, W. Yu, J. Yan, Z. Deng and K. Hong, *Org. Lett.*, 2021, **23**, 1525-1529.
36. L. Jiang, X. Zhang, Y. Sato, G. Zhu, A. Minami, W. Zhang, T. Ozaki, B. Zhu, Z. Wang, X. Wang, K. Lv, J. Zhang, Y. Wang, S. Gao, C. Liu, T. Hsiang, L. Zhang, H. Oikawa and X. Liu, *Org. Lett.*, 2021, **23**, 4645-4650.
37. K. D. Clevenger, J. W. Bok, R. Ye, G. P. Miley, M. H. Verdan, T. Velk, C. Chen, K. Yang, M. T. Robey, P. Gao, M. Lamprecht, P. MP. Thomas, M. N. Islam, J. M. Palmer, C. C. Wu, N. P. Keller, and N. L. Kelleher, *Nat. Chem. Biol.*, 2017, **13**, 895-901.
38. L. Jiang, G. Zhu, J. Han, C. Hou, X. Zhang, Z. Wang, W. Yuan, K. Lv, Z. Cong, X. Wang, X. Chen, L. Karthik, H. Yang, X. Wang, G. Tan, G. Liu, L. Zhao, X. Xia, X. Liu, S. Gao, L. Ma, M. Liu, B. Ren, H. Dai, R. J. Quinn, T. Hsiang, J. Zhang, L. Zhang and X. Liu, *Appl. Microbiol. Biotechnol.*, 2021, **105**, 5407-5417.
39. Z. Quan, A. Hou, B. Goldfuss and J. S. Dickschat, *Angew. Chem. Int. Ed.*, 2022, **61**, e202117273.
40. D. Li, M. Yang, R. Mu, S. Luo, Y. Chen, W. Li, A. Wang, K. Guo, Y. Liu and S. Li, *Chin. Chem. Lett.*, 2023, **34**, 107469.
41. Y. Qiao, Q. Xu, Z. Huang, X. Chen, X. Ren, W. Yuan, Z. Guan, P. Li, F. Li, C. Xiong, H. Zhu, C. Chen, L. Gu, Y. Zhou, C. Qi, Z. Hu, J. Liu, Y. Ye and Y. Zhang, *Org. Chem. Front.*, 2022, **9**, 5808-5818.

42. D. Yan, J. Arakelyan, T. Wan, R. Raina, T. K. Chan, D. Ahn, V. Kushnarev, T. K. Cheung, H. C. Chan, I. Choi, P. Y. Ho, F. Hu, Y. Kim, H. L. Lau, Y. L. Law, C. S. Leung, C. Y. Tong, K. K. Wong, W. L. Yim, N. S. Karnaukhov, R. Y. C. Kong, M. V. Babak and Y. Matsuda, *Acta Pharm. Sin. B.*, 2024, **14**, 421-432.
43. S. Z. Liu, W. J. Wang, Q. P. Liu, M. Yao, L. X. Liao, S. B. Gao, Y. Yu and X. L. Yang, *Org. Lett.*, 2024, **26**, 4475-4479.
44. T. Toyomasu, M. Tsukahara, A. Kaneko, R. Niida, W. Mitsuhashi, T. Dairi, N. Kato, and T. Sassa, *Proc. Natl. Acad. Sci. U. S. A.*, 2007, **104**, 3084-3088.
45. A. Minami, N. Tajima, Y. Higuchi, T. Toyomasu, T. Sassa, N. Kato and T. Dairi, Bioorg. *Med. Chem. Lett.*, 2009, **19**, 870-874.
46. G. Bian, J. Rinkel, Z. Wang, L. Lauterbach, A. Hou, Y. Yuan, Z. Deng, T. Liu and J. S. Dickschat, *Angew. Chem. Int. Ed.*, 2018, **57**, 15887-15890.
47. M. Xu, M. Jia, Y. J. Hong, X. Yin, D. J. Tantillo, P. J. Proteau and R. J. Peters, *Org. Lett.*, 2018, **20**, 1200-1202.
48. T. Toyomasu, A. Kaneko, T. Tokiwano, Y. Kanno, Y. Kanno, R. Niida, S. Miura, T. Nishioka, C. Ikeda, W. Mitsuhashi, T. Dairi, T. Kawano, H. Oikawa, N. Kato, and T. Sassa, *J. Org. Chem.*, 2009, **74**, 1541-1548.
49. T. Mitsuhashi, T. Kikuchi, S. Hoshino, M. Ozeki, T. Awakawa, S. P. Shi, M. Fujita and I. Abe, *Org. Lett.*, 2018, **20**, 5606-5609.
50. T. Shiina, K. Nakagawa, Y. Fujisaki, T. Ozaki, C. Liu, T. Toyomasu, M. Hashimoto, H. Koshino, A. Minami, H. Kawaide and H. Oikawa, *Biosci. Biotechnol. Biochem.*, 2019, **83**, 192-201.
51. L. Jiang, K. Lv, G. Zhu, Z. Lin, X. Zhang, C. Xing, H. Yang, W. Zhang, Z. Wang, C. Liu, X. Qu, T. Hsiang, L. Zhang and X. Liu, *Synth. Syst. Biotechnol.*, 2022, **7**, 1142-1147.
52. P. Zhang, G. Wu, S. C. Heard, C. Niu, S. A. Bell, F. Li, Y. Ye, Y. Zhang and J. M. Winter, *Org. Lett.*, 2022, **24**, 7037-7041.
53. F. Li, S. Lai, W. Yuan, Z. Chen, Z. Guan, C. Chen, H. Zhu, Y. Zhou, J. M. Winter, Z. Xiang, J. Liu, Y. Ye and Y. Zhang, *Org. Lett.*, 2024, **26**, 1734-1738.
54. J.-Y. Liu, F.-L. Lin, K. A. Taizoumbe, J.-M. Lv, Y.-H. Wang, G.-Q. Wang, G.-D. Chen, X.-S. Yao, D. Hu, H. Gao and J. S. Dickschat, *Angew. Chem. Int. Ed.*, e202407895.
55. H. Tao, L. Lauterbach, G. K. Bian, R. Chen, A. W. Hou, T. Mori, S. Cheng, B. Hu, L. Lu, X. Mu, M. Li, N. Adachi, M. Kawasaki, T. Moriya, T. Senda, X. H. Wang, Z. X. Deng, I. Abe, J. S. Dickschat and T. G. Liu, *Nature*, 2022, **606**, 414-419.